Intrinsic Polymer Dielectrics for High Energy Density and Low Loss Electric Energy Storage

Junji Wei [a,b,*] and Lei Zhu [c,*]

[a] *Institute of Polymer Materials, School of Materials Science and Engineering, Chang'an University, Xi'an 710064, Shaanxi, P. R. China*

[b] *Engineering Research Center of Transportation Materials, Ministry of Education, Chang'an University, Xi'an 710064, P. R. China*

[c] *Department of Macromolecular Science and Engineering, Case Western Reserve University, Cleveland, Ohio 44106-7202, United States*

* Corresponding authors. Emails: weijj@chd.edu.cn (J. Wei) and lxz121@case.edu (L. Zhu)

Abstract

High energy density, high temperature, and low loss polymer dielectrics are highly desirable for electric energy storage, e.g., film capacitors in the power electronics of electric vehicles and high-speed trains. Fundamentally, high polarization and low dielectric loss are two conflicting physical properties, because more polarization processes will involve more loss mechanisms. As such, we can only achieve a delicate balance between high dielectric constant and reasonably low loss. This review focuses on achieving low dielectric loss while trying to enhance dielectric constants for dielectric polymers, which can be divided into two categories: extrinsic and intrinsic. For extrinsic dielectric systems, the working mechanisms include dipolar (e.g., nanodielectrics) and space charge (e.g., ion gels) interfacial polarizations. These polarizations do not increase the intrinsic dielectric constants, but cause decreased breakdown strength and increased dielectric loss for polymers. For intrinsic dielectric polymers, the dielectric constant originates from electronic, atomic (or vibrational), and orientational polarizations, which are intrinsic to the polymers themselves. Because of the nature of molecular bonding for organic polymers, the dielectric constant from electronic and atomic polarizations is limited to 2-5 for hydrocarbon-based insulators (i.e., band gap > 4 eV). It is possible to use orientational polarization to enhance intrinsic dielectric constant while keeping reasonably low loss. However, nonlinear ferroelectric switching in ferroelectric polymers must be avoided. Meanwhile, paraelectric polymers often exhibit high electronic conduction due to large chain motion in the paraelectric phase. In this sense, dipolar glass polymers are more attractive for low loss dielectrics, because frozen chain dynamics enables deep traps to prevent electronic conduction. Both side-chain and main-chain dipolar glass polymers are promising candidates. Furthermore, it is possible to combine intrinsic and extrinsic dielectric properties synergistically in multilayer

films to enhance breakdown strength and further reduce dielectric loss for high dielectric constant polar polymers. At last, future research directions are briefly discussed for the ultimate realization of next generation polymer film capacitors.

Keywords: Electric energy storage; intrinsic polymer dielectrics; extrinsic polymer dielectrics; orientational polarization; ferroelectric polymers; paraelectric polymers; dipolar glass polymers; multilayer films

Contents

Nomenclature

ArPTU	Aromatic polythiourea
BDS	Broadband dielectric spectroscopy
BOPP	Biaxially oriented polypropylene
BR	Bruggeman model
CEP	Cyanoethylated pullulan
CN-PDPMA	Cyanoethylated poly(2,3-dihydroxylpropyl methacrylate)
CN-PVA	Cyanoethylated poly(vinyl alcohol)
CuPc	Copper phthalocyanine
D-E loop	Electric displacement-electric field loop
DFT	Density functional theory
DGP	Dipolar glass polymer
EDL	Electric double layer
[EMIM][TFSI]	1-Ethyl-3-methylimidazolium bis(trifluoromethylsulfonyl) imide
FETs	Field effect transistors
HN	Havriliak-Negami deconvolution method
LDPE	Low-density polyethylene
MD	Molecular dynamics
MG	Maxwell Garnett method
nAl	Nano-aluminum
P3HT	Poly(3-hexyl thiophene)
PBCMO	Poly[3,3-bis(chloromethyl)oxetane]
PC	Polycarbonate

PECH	Polyepichlorohydrin
PEI	Polyetherimide
PEO	Poly(ethylene oxide)
PI	Polyimide
PMMA	Poly(methyl methacrylate)
PMSEMA	Poly[2-(methylsulfonyl)ethyl methacrylate
POSS	Polyhedral oligomeric selsisquioxane
PP	Polypropylene
PS	Polystylene
PSF	Polysulfone
PVDF	Poly(vinylidene fluoride)
P(VDF-HFP)	Poly(vinylidene fluoride-*co*-hexafluoropropylene)
P(VDF-TrFE)	Poly(vinylidene fluoride-*co*-trifluoroethylene)
P(VDF-TrFE-CTFE)	Poly(vinylidene fluoride-*co*-trifluoroethylene-*co*-chlorotrifluoroethylene)
SO_2-PPO	Sulfonylated poly(2,6-dimethyl-1,4-phenylene oxide)
TEM	Transmission electron microscope
α_a	Atomic polarizability
α_e	Electronic polarizability
A	Area of the film sample
C^*_{elect}	Capacitance from conduction of electrons
C^*_{ion}	Capacitance from conduction of ions
C^*_{inj}	Capacitance from injected homo-charges via the conduction pathways

C_p	Capacitance
C^*_{sam}	Sample capacitance
C_{str}	Stray capacitance
d	Thickness of the film sample
D	Electric displacement
D_{film}	Electric displacement of the film
E_0	External electric field
E_c	Coercive field
E_L	Local electric fields.
ε_0	Vacuum dielectric constant
ε_{eff}	Effective dielectric constant
ε_m	Dielectric constant of the matrix
ε_p	Dielectric constant of the fillers
ε_r or κ	Relative dielectric constant
ε_{rs}	Static dielectric constant
$\varepsilon_{r\infty}$	Dielectric constant at high frequencies
ϕ	Volume fractions
f	Frequency
g	Correlation factor
η	Volume fraction of fillers
k	Boltzmann constant
μ	Dipole moment
M	Molecular weight of the polymer repeat unit

N_A	Avogadro's number
n_{dip}	Concentrations of dipoles
N_{ind}	Density of induced dipoles by electronic and atomic polarizations
n_{sp}	Concentrations of charge carriers
P_s	Spontaneous polarization
ρ	Density of the polymer
σ	Electronically conductive
σ_{dip}	Dipolar interfacial polarization
σ_{sp}	Space charge polarization
T	Temperature
$\tan\delta$	Dissipation factor
T_g	Glass transition temperature
T_m	Melting temperature
V	Volume
V(t)	Applied sinusoidal voltage
ω	Angular frequency
x_{NL}	Content of the nonlinear component

1. Introduction

Electric energy storage is of vital importance for green and renewable energy applications. Different from batteries, which have a high energy density via electrochemical reactions, capacitors physically store and discharge electric energy within a very short time. In this sense, capacitors have a high power density and are ubiquitous in all large-scale electrical and power devices. Recently, further development for capacitor technologies is demanded by new applications,[1-4] including electric vehicles, high speed trains, smart power grids, and even electric ships and airplanes. Compared to ceramic[5] and electrolytic capacitors,[6] polymer film capacitors have certain advantages, including stable capacitance, high voltage, high ripple current, self-healing, low loss, and ultrahigh power density.[1, 2] Current state-of-the-art polymer film for capacitors is the biaxially oriented polypropylene (BOPP) film. This is primarily owing to its ultralow dielectric loss (e.g., dissipation factor, $\tan\delta \sim 0.0003$), high dielectric breakdown strength (> 700 MV/m), and long lifetime (> 20,000 h) due to the self-healing merit.[7, 8] Note that the most important requirement for capacitor films is not necessarily high energy density, but low dielectric loss to avoid significant heat generation in wound capacitors.[1, 9] Without any sacrifice of breakdown strength and lifetime, the polymer film should be as thin as possible to achieve a higher volumetric capacitance density [$C_p/V = \varepsilon_r\varepsilon_0/d^2$, where C_p is capacitance, V is volume, ε_r and ε_0 are relative and vacuum dielectric constant (or permittivity, κ) and d is the film thickness] and thus a lower material cost. At present, the thinnest BOPP film is 2.5 μm with a capacitance density of 3.2 F/m^3, and the cost of metallized films is about $20-30/kg.

However, the temperature rating for BOPP film capacitors is only 85 °C, above which the capacitor lifetime tends to decrease. As such, BOPP film capacitors cannot be directly used in the high temperature environment (~140 °C) of modern power electronics, which use silicon- or

wide bandgap semiconductor-based transistors.[10-12] A 60-70 °C water-cooling system is then necessary to cool BOPP film capacitors, and this incurs additional costs. To develop next generation capacitor films, the following technological and scientific considerations should be carefully taken into account. First, the new polymer film should withstand at least 140 °C with a low dielectric loss ($\tan\delta < 0.003$). In this way, the water-cooling system may be eliminated to save cost for the system. Second, the new polymer film should be able to self-heal to guarantee a long lifetime. Third, film capacitors occupy nearly half of both volume and cost of the power electronic unit. To achieve similar or even lower prices as the metallized BOPP films, the new polymer film should have a higher energy density for miniaturization. Based on the cost-saving consideration, the polymer films should be as thin as ~3 μm in order to compete with the 2.5 μm BOPP film technology. This will require biaxial film orientation using the tenter-line processing.[13]

In this review, we will not be able to cover all the above aspects for next-generation polymer dielectric films for electric energy storage. Instead, we will only focus on enhancing energy density via multiple polarization mechanisms for miniaturization, while keeping low dielectric loss. Meanwhile, we will also briefly discuss high temperature polymer dielectrics. Different polarization mechanisms include electronic (10^{15}-10^{18} Hz), atomic (or vibrational, 10^{12}-10^{15} Hz), orientational (typically 10^{3}-10^{9} Hz), and space charge polarizations ($<10^{4}$ Hz).[14] From the fundamental physics point of view, high polarization/dielectric constant and ultralow dielectric loss ($\tan\delta < 0.001$) are contradictory material properties and cannot be achieve simultaneously, because more polarization processes will incur more dielectric loss mechanisms. Therefore, we can only optimize the system to achieve a relatively high energy density (e.g., ~10 J/cm^3) with a reasonably low dielectric loss (e.g., $\tan\delta < 0.003$).

It is known that the energy density is proportional to the dielectric constant and square of the applied electric field; therefore, it seems more beneficial to increase the electric field for high energy density. However, given the already high breakdown strength for dielectric polymer films (e.g., >700 MV/m for BOPP)[15] and the record breakdown strength is about 2 GV/m (e.g., single crystal diamond),[16, 17] the room for increasing the operating field without decreasing the lifetime is rather limited. Meanwhile, it is not a good idea to run polymer film capacitors under high electric fields, because their dielectric lifetime will substantially decrease. Therefore, increasing dielectric constant is more reasonably achievable for polymers.[18-20] On the basis of different polarization mechanisms, polymers can be divided into intrinsic and extrinsic dielectrics. An intrinsic polymer dielectric has a genuine dielectric constant based on electronic, atomic, and orientational polarizations. An extrinsic polymer dielectric has various interfacial polarizations, which do not increase the intrinsic dielectric constant. Although both types of polymer dielectrics can seemingly increase the capacitance and thus electric energy storage, extrinsic interfacial polarizations can cause various issues. In the following, we will discuss both extrinsic and intrinsic polymer dielectrics, and suggest viable intrinsic dielectric polymers for high energy and low loss dielectric capacitor applications.

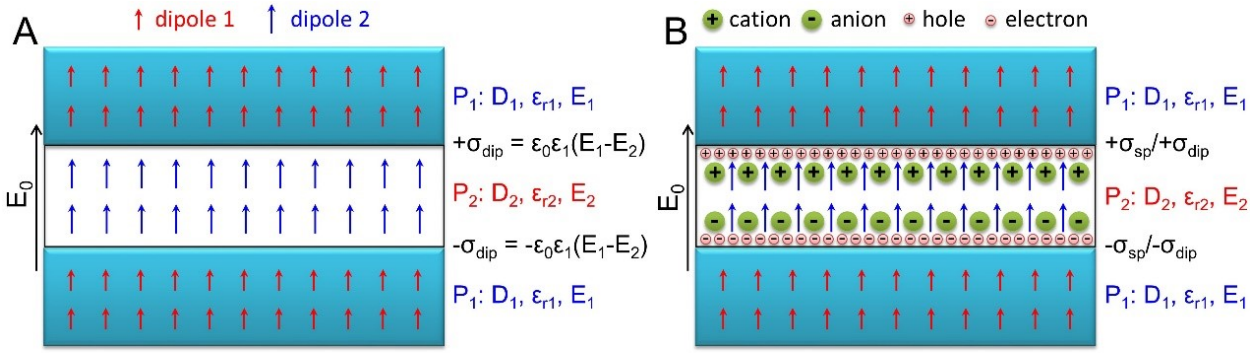

Fig. 1. Schematic representation of interfacial polarizations (A) without and (B) with space charge polarization (σ_{sp}). E_0 is the applied electric field. D_i, ε_{ri}, and E_i are electric displacement, relative permittivity, and nominal electric field for the polymer *i* [*i* is 1 for polymer 1 (P_1) and 2

for polymer 2 (P_2)]. σ_{dip} is the dipolar interfacial polarization based on electronic, atomic, and orientational polarizations. For insulators, there should only exist thermally activated electrons, and no free holes. The holes at the P_1/P_2 interface represent image charges for the polarized electrons at the P_2/P_1 interface.

2. Extrinsic dielectric polymers based on interfacial polarizations

For a multicomponent system under an applied electric field (E_0), interfacial polarizations can happen when different components have different dielectric constants and/or bulk conductivities.[14, 18] We can explain this using a layered geometry with polymer 2 (P_2) sandwiched by polymer 1 (P_1); see Fig. 1. We assume that relative dielectric constants for P_1 and P_2 are $\varepsilon_{r1} < \varepsilon_{r2}$, and P_2 is more conductive than P_1. Because of the non-uniform electric field distribution in multicomponent systems,[14, 18] the nominal electric field in P_1 (E_1) is higher than that in P_2 (E_2). In the first case (Fig. 1A), there is no space charge polarization (σ_{sp}), but only dipolar interfacial polarization (σ_{dip}) based on the difference in electronic, atomic, and orientational polarizations for P_1 and P_2. Under the equal electric displacement condition: $D_1 = \varepsilon_{r1}\varepsilon_0 E_1 = D_2 = \varepsilon_{r2}\varepsilon_0 E_2$, the dipolar interfacial polarization can be derived: $\sigma_{dip} = \varepsilon_{r1}\varepsilon_0(E_1-E_2)$. In the second case (Fig. 1B), there is a finite σ_{sp} from polarization of charge carriers (i.e., ions and thermally activated electrons). Note that there should not exist any free holes for an insulating polymer. The holes at the P_1/P_2 interface are drawn in Fig. 1B as image charges to compensate the polarized electrons at the P_2/P_1 interface. Polarization of charge carriers in P_2 will generate a negative internal electric field, thus decreasing the electric field in P_2 (E_2). In turn, the electric field in P_1 (E_1) will increase. Eventually, the system reaches an equilibrium with finite σ_{sp} and σ_{dip}. In general, σ_{dip} increases with the applied field E_0, whereas σ_{sp} saturates at a high enough field by complete polarization of all polarizable charge carriers in P_2. Depending on the concentrations of charge carriers (n_{sp}) and dipoles (n_{dip}) in P_2, two situations can take place. When n_{sp} is much lower than n_{dip} such as in conventional dielectrics with a small amount (e.g., < 1 ppm) of impurity ions,[21-

23] σ_{dip} will be greater than σ_{sp} at high fields. When n_{sp} is comparable to n_{dip}, such as in polymeric ion gels,[24, 25] σ_{sp} will be significantly ($>10^3\times$) higher than σ_{dip} due to formation of the electric double layer (EDL).[26, 27]

It is worth noting that these interfacial polarizations, especially σ_{sp}, increase the overall capacitance (C_p), but not the intrinsic dielectric constants of polymers (i.e., ε_{r1} and ε_{r2} for P_1 and P_2, respectively). Therefore, we call these multicomponent systems as extrinsic polymer dielectrics.

2.1. Polymer nanocomposite dielectrics (or nanodielectrics)

The first example of extrinsic dielectric polymers is a nanocomposite dielectric or a nanodielectric, which is comprised of a polymer matrix and inorganic nanofillers.[28-35] The nanofillers can be either insulating (e.g., ceramics) or conductive (e.g., metals or carbon nanotubes/graphenes). A great deal of work has been done in this area to study the relationship between dielectric properties of nanodielectrics and their components, including size, shape, composition, and dispersion of fillers. Compared with the polymer matrix, the apparent dielectric constant of these nanodielectrics is improved, ranging from several to tens of times. For polymer nanodielectrics with spherical fillers, there are two fundamental models (or mixing rules) to predict the dielectric constant. They are Maxwell Garnett model and Bruggeman model.[28, 36] The working principle is actually the dipolar interfacial polarization. Before introducing these two mixing rules, we introduce parallel and series capacitor models first, which are two extreme cases for mixed dielectrics.

For the parallel capacitor model, the complex dielectric constant (ε_r^*) is expressed as follows:

$$\varepsilon_r^* = \varepsilon_{r1}^* \phi_1 + \varepsilon_{r2}^* \phi_2 \quad (1)$$

where ϕ_1 and ϕ_2 are volume fractions and ε_{r1}^* and ε_{r2}^* are dielectric constants of the polymer matrix and fillers. For the series capacitor model, ε_r^* is expressed as:

$$\frac{1}{\varepsilon_r^*} = \frac{\phi_1}{\varepsilon_{r1}^*} + \frac{\phi_2}{\varepsilon_{r2}^*} \quad (2)$$

The parallel capacitor model represents one extreme of the most effective enhancement of dielectric constant for nanodielectrics, whereas the series capacitor model represents the other extreme of the least effective enhancement of dielectric constant.

For the Maxwell Garnett (MG, or Maxwell-Wagner) model, the effective dielectric constant [$\varepsilon_{eff}(MG)$] is expressed as:

$$\varepsilon_{\text{eff}}(MG) = \varepsilon_{\text{m}} \frac{2\varepsilon_m + \varepsilon_{\text{p}} + 2\eta\Delta\varepsilon}{2\varepsilon_{\text{m}} + \varepsilon_{\text{p}} - \eta\Delta\varepsilon} \quad (3)$$

where ε_m and ε_p are dielectric constant of the matrix and fillers, $\Delta\varepsilon = \varepsilon_p - \varepsilon_m$, and η is the volume fraction of fillers. For the Bruggeman (BR) model, the effective dielectric constant [$\varepsilon_{eff}(BR)$] is expressed as:

$$\varepsilon_{\text{eff}}(BR) = \frac{1}{4}\left(\Delta\varepsilon(3\eta - 2) + \varepsilon_{\text{P}} + \sqrt{[\Delta\varepsilon(2 - 3\eta) - \varepsilon_{\text{P}}]^2 + 8\varepsilon_{\text{m}}\varepsilon_{\text{p}}}\right) \quad (4)$$

If we assume the $\varepsilon_m = 3$ and $\varepsilon_p = 200$, then we can see the difference among the above four mixing rules as a function of the volume fraction of particular fillers. As shown in Fig. 2A, the parallel and series capacitor models are two extreme cases. These could be tested in polycarbonate (PC)/poly(vinylidene fluoride-*co*-hexafluoropropylene) [P(VDF-HFP)] multilayer films and blends.[37] As shown in Fig. 1B, dielectric constants of the PC/P(VDF-HFP) multilayer films fit well with the prediction by the series capacitor model. Dielectric constants of the PC/P(VDF-HFP) blends lie between those of the series and the parallel capacitor models. This is because the parallel capacitor model cannot represent the immiscible blends.

Generally speaking, the MG model is applicable to a composite with a low loading of spherical fillers. Only enhancement of the local field between two poles of the filler is taken into account. The coupling effect among neighboring fillers is neglected. Different from the MG model, the BR model considers the dipole-dipole coupling effect among neighboring fillers in the composite. Namely, the BR model is more suitable for the nanocomposites with a higher content of fillers. Consequently, the BR model is more effective in enhancing ε_{eff} (Fig. 2A). As shown in Fig. 2C, the BR model fits the experiment broadband dielectric spectroscopy (BDS) data of polypropylene (PP)/$BaTiO_3$ and PP/$BaTiO_3$@polyhedral oligomeric selsisquioxane (POSS) nanocomposites reasonably well,[38] whereas the MG model significantly underestimates the apparent dielectric constant. In a recent study, Elshad et al. used coarse-grained molecular dynamics (MD) simulation to support this conclusion.[36] It was found that the dipole-dipole coupling effect became important and could not be ignored at high filler contents. After considering the influence of dipolar correlation effects, the simulation result, as well as the BR model, fit the experiment data well. On the contrary, the MG model underestimated the ε_{eff}.

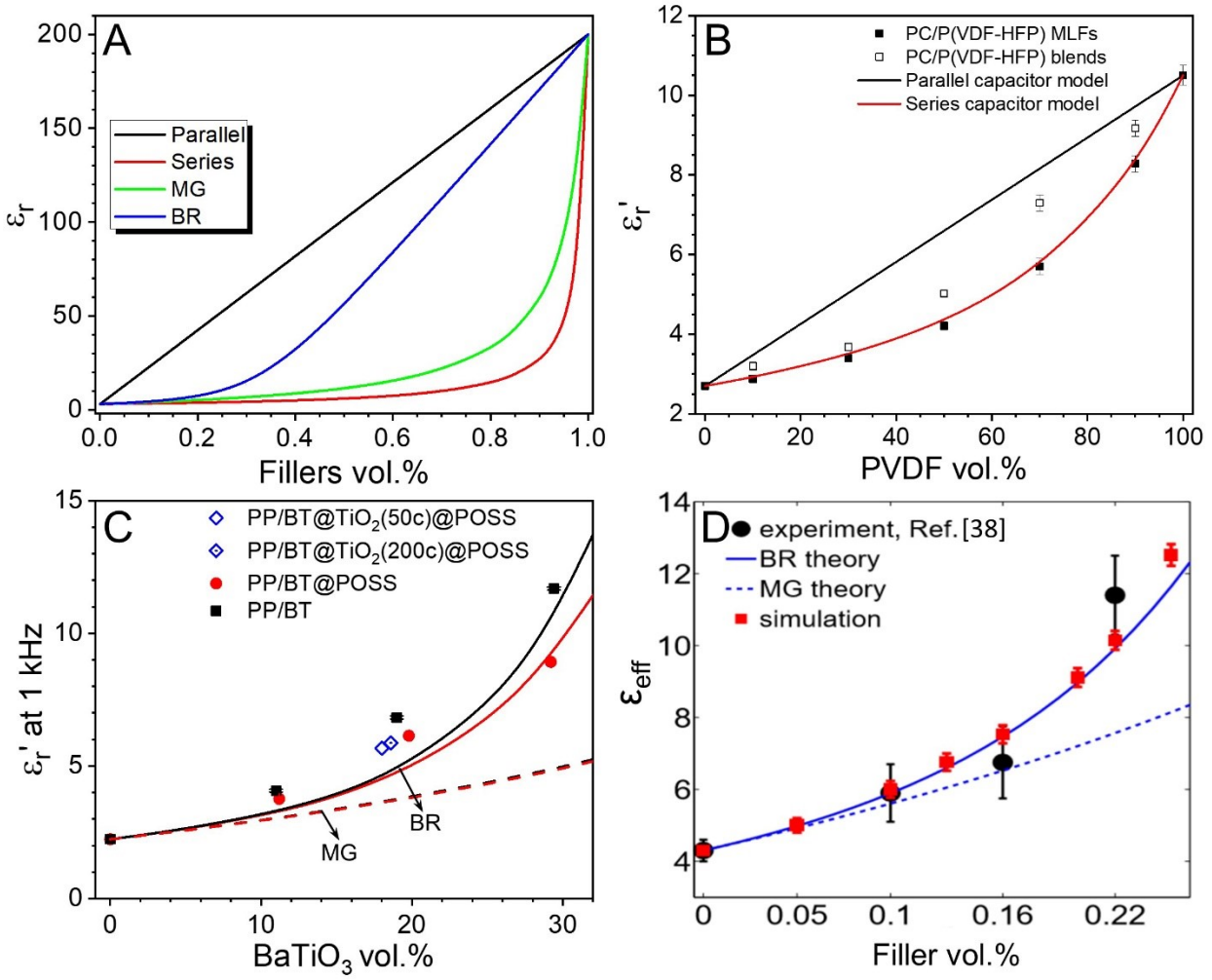

Fig. 2. (A) Predicted ε_r with four mixing rules, including parallel and series capacitor models, MG model, and BR model at different filler volume fractions, assuming $\varepsilon_p = 200$ and $\varepsilon_m = 3$. (B) Dielectric constant as a function of PVDF vol.% for the PC/P(VDF-HFP) blend and multilayer films.[36] Copyright 2019. Adopted with permission from Elsevier Science Ltd. (C) The ε_r' for PP/$BaTiO_3$, PP/$BaTiO_3$@POSS, and PP/$BaTiO_3$@TiO_2@POSS 80/20 nanocomposites as a function of volume fraction of $BaTiO_3$ nanoparticles measured at 1 kHz and RT.[37] Copyright 2016. Adopted with permission from American Chemical Society. (D) Dependence of ε_{eff} on the filler content, η, in the random composite. The experimental result is from Ref. [39].[35] Copyright 2016. Adopted with permission from Royal Society of Chemistry.

As we can see from Fig. 2, the dielectric constant of nanodielectrics cannot be effectively enhanced for spherical fillers, unless the percolation threshold of 35-40 vol.% is reached.[40, 41] For example, when Li and Ti-codoped NiO was added into PVDF, the composite showed an apparent ε_r' as high as 90 at 100 Hz with the filler loading reaching 40 vol.%.[42] Arbatti et al.

produced a calcium copper titanate/P(VDF-TrFE) (TrFE is trifluoroethylene) composite with an apparent ε_r' of ~610 at 50 vol.% filler content at 100 Hz.[43] Dang et al. prepared a high κ (Ni-$BaTiO_3$)/PVDF nanocomposite, which exhibited a high apparent permittivity of 800 at a $BaTiO_3$ fraction of ~40 vol.%.[44] With such a high inorganic filler content, the nanodielectrics lose the melt processability for polymers. This can cause additional issues. 1) It is difficult to achieve uniform dispersion of nanoparticles in the polymer matrix because of strong van der Waals interaction at the nanoscale, unless the polymers are directly grafted onto the nanoparticles.[45] 2) The mechanical strength and elongation at break of nanocomposite films significantly deteriorate when the filler content gets close to the percolation threshold. 3) The thickness of nanodielectric films is limited by the size of fillers and cannot be too thin. 4) Nanodielectrics are not suitable for biaxial orientation, which is a typical process for industrial production of capacitor films. Because of poor interfacial adhesion between the particles and the polymer matrix, cavitation can easily happen upon stretching.

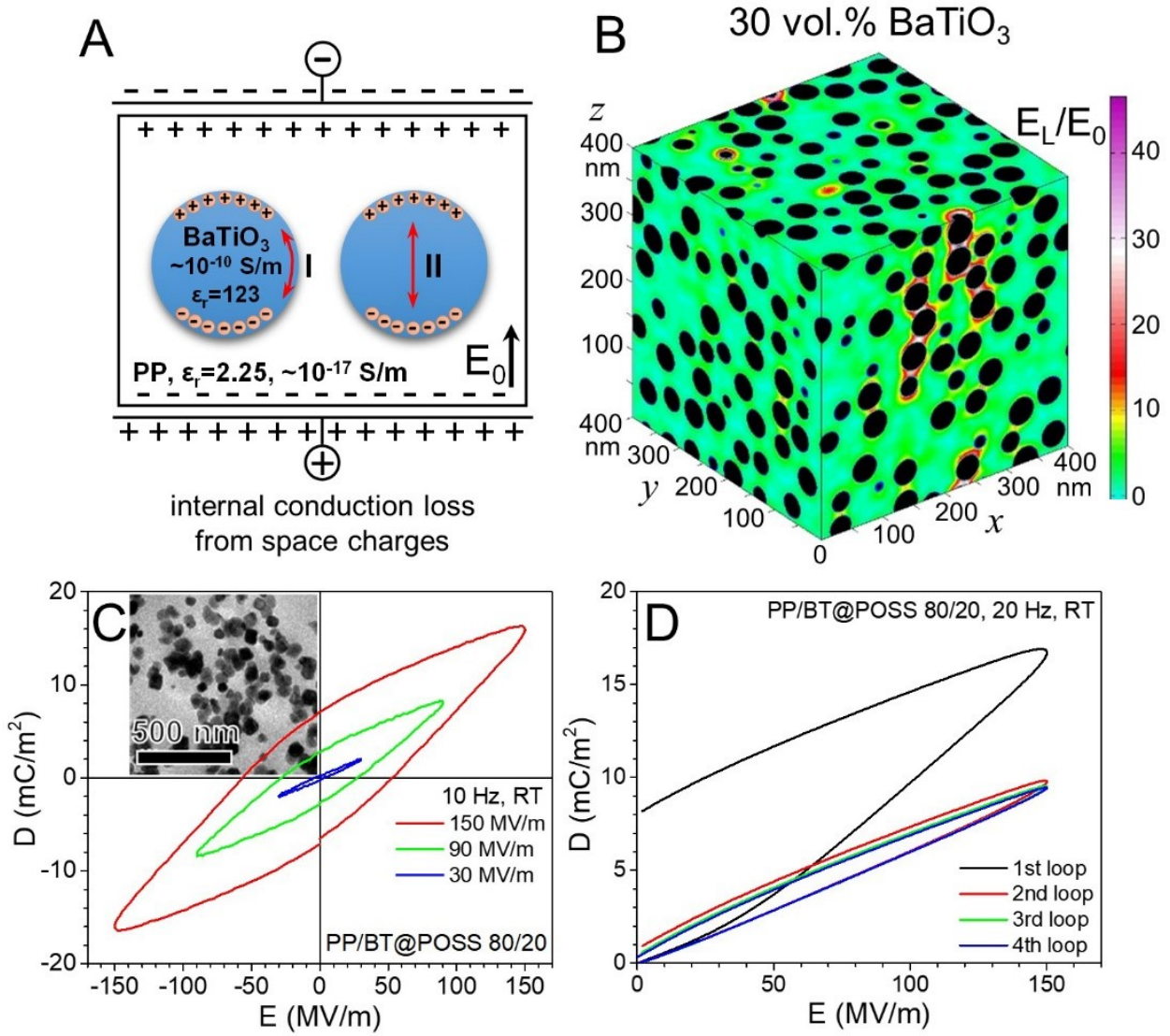

Fig. 3. (A) Schematic representation of internal conduction loss mechanism from space charges in $BaTiO_3$ nanoparticles. (B) Electric field distribution (E_L/E_0) in the matrix of a PP/$BaTiO_3$ 70/30 (vol./vol.) nanocomposite. E_L and E_0 are the local and the external electric fields. (C) Bipolar D-E loops for the PP/$BaTiO_3$@POSS 80/20 (vol./vol.) nanocomposite. The inset shows a TEM image of the nanodielectric. (D) Consecutive four unipolar D-E loops for the PP/$BaTiO_3$@POSS 80/20 (vol./vol.) nanocomposite at room temperature.[37] Copyright 2016. Adopted with permission from American Chemical Society.

In addition to the above processing difficulties, these nanodielectrics often exhibit a unique loss mechanism, as depicted in Fig. 3A.[38] As we know, ferroelectric ceramics such as $BaTiO_3$ are more electronically conductive ($\sigma \sim 10^{-10}$ S/m) than dielectric polymers. This is largely because of the high dielectric constant ($\varepsilon_r = 123$ in this case), which enables thermally activated

electrons. Upon electric poling, these thermally activated electrons will accumulate at the PP/$BaTiO_3$ interface along the field direction, because PP is much more insulating ($\sigma \sim 10^{-17}$ S/m). Here, the positive charges in Fig. 3A are image charges to compensate the polarized electrons. Upon bipolar poling, these interfacial charges will reverse the polarity via either the interface (I) or the bulk (II) of the $BaTiO_3$ particle (Fig. 3A). As a result, significant hysteresis loop loss from internal conduction is observed for the PP/$BaTiO_3$ 80/20 nanocomposite [see the electric displacement-electric field (D-E) loops and the inset transmission electron microscope (TEM) image in Fig. 3C]. However, the situation is different for repetitive unipolar poling as shown in Fig. 3D. Only the first unipolar loop shows a large hysteresis loop loss, and the rest loops become slim. This is because the interfacial charges are always poled in the same direct, and the polarity is never reversed for the second to fourth loops. In this sense, nanodielectrics can only be used in DC, rather than AC applications. To mitigate the problem of internal conduction loss, much more insulating ceramics such as Al_2O_3 should be used; however, insulating ceramics usually have a rather low dielectric constant.

Furthermore, it is observed that nanodielectrics easily breakdown upon electric poling. The main reason is attributed to the nonuniform electric field distribution in multicomponent systems, as long as there is a large permittivity contrast between the fillers ($\varepsilon_{r,f}$) and the polymer matrix ($\varepsilon_{r,m}$). Basically, the high κ inorganic fillers bear a low electric field, E_f, and the low κ polymer matrix bears a high electric field, E_m.[36] From a computer simulation of the nanodielectric with a random particle distribution, the local E_m could be a few to several tens of times higher than the applied electric field (E_0), especially between the aligned particles along the electric field direction (Fig. 3B).[38, 46] As such, “hot spots” are created in the polymer matrix, which can be easy to breakdown electrically. The reason is attributed to the high dipolar

interfacial polarization because of the large difference in dielectric constants between the fillers and the polymer (similar to the case in Fig. 1A).[36] This result is important, because it also explains why nanodielectrics with particle aggregation have even lower breakdown strengths, because the local field between aggregated particles is even higher than that between dispersed particles. One way to mitigate this problem is to decrease the permittivity contrast by lowering the dielectric constant of ceramic fillers, such as Al_2O_3 ($\varepsilon_r = 9$)[47] and TiO_2 ($\varepsilon_r \sim 40$ for the anatase form);[48] however, this will decrease the ε_{eff} of the nanodielectric.

How to ultimately solve the above problems for nanodielectrics? The ideal solution is to decrease the filler content as much as possible, while still achieving a large enhancement effect on dielectric properties (e.g., dielectric constant and breakdown strength) for the nanodielectrics. Recently, Thakur et al. developed a novel nanocomposite approach, where the filler content was less than 1 vol.%.[49] Surprisingly, significant improvement of the ε_{eff} (up to 50%) and dielectric breakdown strength are observed. For example, after adding only 0.32 vol.% of Al_2O_3 nanoparticles into polyetherimide (PEI), the ε_{eff} of the nanocomposite could be as high as ~5.0, which was 55% higher than that (3.2) of the neat PEI. The discharged energy density achieved as high as ~2.9 J/cm^3 under 300 MV/m at room temperature. Meanwhile, breakdown strength could also be enhanced. For example, the DC breakdown strength of low density polyethylene (LDPE)/Al_2O_3 nanocomposites with <1 wt.% filler content was enhanced.[50] It was attributed to the reduced volumetric conductivity because of deep trap levels in the nanocomposites.[50, 51] At this moment, more research is needed to testify this concept in other systems and understand the fundamental mechanism/physics for the unusual behavior.

Another type of nanodielectrics utilizes conducting fillers, either metallic [52-54] or carbonaceous particles including carbon nanotubes and graphenes.[55-57] Enhanced ε_{eff} is

reported, as indicated by numerous low-field BDS studies. Meanwhile, the electrical percolation threshold can be lower than the physical percolation threshold.[58, 59] The high dielectric constants, ranging between 100 and a few thousands, can be attributed to partial conductive pathways in direct contact with the metal electrodes, but not penetrating through the entire sample.[60] In this sense, these conductive nanofiller composites behave similar to a supercapacitor with an increased electrode area. Nonetheless, most studies stop at the low-field dielectric characterization. Very few studies proceed to high-field dielectric studies, including leakage current and dielectric breakdown studies. In a recent work, we studied PP nanocomposites with nano-aluminum (nAl) particles (18 and 100 nm).[60] The filler content ranges from 5 to 25 vol.%. After surface grafting of polymer brushes, these nAl particles disperse uniformly in the PP matrix. Because there is no particle aggregation and thus no conductive pathways in direct contact with the metal electrodes, large enhancement of the ε_{eff} is not observed. For example, at 18.5 vol.% nAl, the ε_r is only 4.4 at 1 kHz at room temperature, even smaller than that of 6.1 for the PP/$BaTiO_3$@POSS 80/20 nanocomposite. The breakdown strength for the PP/nAl nanocomposites dramatically decreases upon increasing the nAl content. For example, at 25 vol.% nAl, the breakdown strength is only 30 MV/m, more than 20 times lower than that (630 MV/m) for the neat PP matrix. Through a leakage current study, the mechanism is unraveled. The bulk conductivity for the PP/nAl nanocomposites (e.g., 18.5 vol.% nAl) exhibit three conduction mechanisms. At a low electric field (e.g., <20 MV/m), Ohmic conduction is observed. Between 20 and 35 MV/m, conduction via the hopping mechanism is observed. Above 35 MV/m, Fowler-Nordheim field electron emission is observed with significantly enhanced electronic conduction. Finally, above 70 MV/m, the nanocomposite breaks down catastrophically. From this study, it is clear that tightly packed metallic nanoparticles serve as the electron sources.

When the local field in the dielectric matrix becomes high enough, Fowler-Nordheim field electron emission would happen.[14] Basically, electrons are ejected from the metallic nanoparticles into the polymer matrix, making the entire composite conductive. It is also because of the Fowler-Nordheim emission, bipolar D-E loops are broad. Therefore, we conclude that polymer/conductive filler nanocomposites are not suitable for high energy density capacitor applications. Indeed, the Fowler-Nordheim field electron emission was also observed in other polymer/metallic nanoparticle composites.[61-64] These composite films were used as electrical switches, rather than capacitor films.

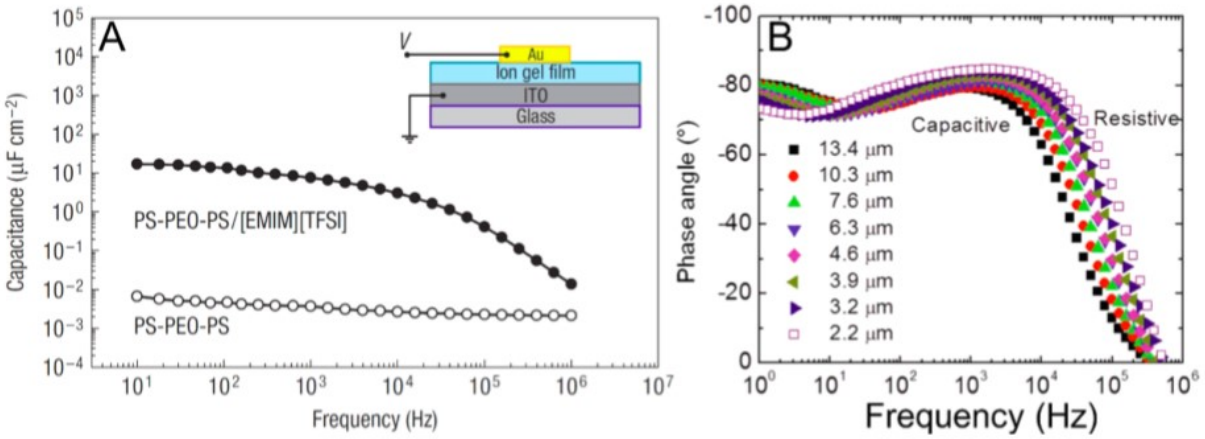

Fig. 4. (A) Specific capacitance of a PS-*b*-PEO-*b*-PS triblock copolymer and its ion gel with the [EMIM][TFSI] ionic liquid as a function of frequency.[64] Copyright 2008. Reproduced with permission from Nature Publishing Group. (B) Impedance phase angle as a function of frequency for a PS-*b*-PMMA-*b*-PS/[EMIM][TFSI] ion gel with different thicknesses.[65] Copyright 2011. Reproduced with permission from American Chemical Society.

2.2. Ion gel polymer dielectrics

Space charge polarization can also improve the capacitance of polymer dielectrics. In a broader scope, space charges can include electrons, holes, and positive/negative ions. For electrons and holes, they often exist in semiconductors. In this review, we consider that

semiconductors are outside the scope, and will not be discussed any further. We will focus on polymer dielectrics containing ions. Because ions can be blocked by metallic electrodes, polymer electrolytes can survive relatively high electric fields. A successful example is the ion gel, where the EDL plays an important role. The specific capacitance of an EDL can be calculated from the Helmholtz model:[26]

$$C_{EDL} = \frac{\varepsilon_r \varepsilon_0}{4\pi\lambda} \quad (5)$$

where ε_r is the permittivity and λ is the thickness of the EDL. Considering the small value of λ (a few nanometers), the C_{EDL} can be much higher than that of neat polymer dielectrics. For example, the specific capacitance for poly(ethylene oxide) (PEO)/$LiClO_4$ can be at least 10^5 times that of PP at 1 Hz.[65] Based on this, ion gels based on block copolymers and ionic liquids could be used as gate dielectrics in field effect transistors (FETs).[25] As shown in Fig. 4A, the specific capacitance of a polystyrene-*b*-PEO-*b*-polystyrene (PS-*b*-PEO-*b*-PS) triblock copolymer and its ion gels with an ionic liquid, 1-ethyl-3-methylimidazolium bis(trifluoromethylsulfonyl) imide ([EMIM][TFSI]), is as high as about 20 μF/cm^2 at 10 Hz, three orders of magnitude higher than that of the pure triblock copolymer.[66] However, the loss of ion gels becomes high for frequency beyond 10^4 Hz. Fig. 4B shows the phase angle as a function of frequency for another ion gels, where the triblock copolymer is PS-*b*-poly(methyl methacrylate)-*b*-PS (PS-*b*-PMMA-*b*-PS) and the ionic liquid is [EMIM][TFSI].[67] The dielectric loss is zero when the impedance phase angle $\varphi = -90^o$. As shown in Fig. 4B, the dielectric loss of these ion gels with different thicknesses reaches the lowest value (i.e., the highest φ) in the range of 10^3~10^4 Hz and increases dramatically above 10^4 Hz. The reason is that ions in the EDL of the ion gel move slowly and cannot catch up with the applied field at high enough frequencies. The slow motion of ions causes significant conduction loss in the EDL. Therefore, ion gels are not suitable for film

capacitors, which operate above 2000 Hz in electric vehicles. Even at low frequencies, the dissipation factor is higher than 0.05 for ion gels because of the slow ion speed in the EDL. Future research needs to focus on reducing the dielectric loss for ions at high frequencies.

3. Intrinsic polymer dielectrics based on electronic, atomic, and orientational polarizations

Intrinsic polymer dielectrics have genuine dielectric constants from electronic, atomic, orientational polarizations. It can be formulated by using the Kirkwood-Fröhlich theory:[14]

$$\frac{(\varepsilon_{rs}-\varepsilon_{r\infty})(2\varepsilon_{rs}+\varepsilon_{r\infty})}{\varepsilon_{rs}(\varepsilon_{r\infty}+2)^2} = \frac{N_{dip}g\mu^2}{9\varepsilon_0 kT} \quad (6)$$

where ε_{rs} is the static dielectric constant, $\varepsilon_{r\infty}$ the dielectric constant at high frequencies (i.e., from electronic and atomic polarizations), N_{dip} the density of orientational molecular dipoles, g the correlation factor, μ the dipole moment, k the Boltzmann constant, and T temperature. The $\varepsilon_{r\infty}$ can be estimated by the Clausius-Mossotti equation:[22]

$$\frac{\varepsilon_{r\infty}-1}{\varepsilon_{r\infty}+2} = \frac{N_{ind}(\alpha_e+\alpha_a)}{3\varepsilon_0} = \frac{\rho N_A(\alpha_e+\alpha_a)}{3\varepsilon_0 M} \quad (7)$$

where N_{ind} is the density of induced dipoles by electronic and atomic polarizations, α_e and α_a the electronic and atomic polarizability, N_A the Avogadro's number, ρ the density of the polymer, and M the molecular weight of the polymer repeat unit. Starting from the measurement issues, we will discuss viable approaches to enhance intrinsic dielectric constants of dielectric polymers for high density and low loss electric energy storage.

3.1. Measurement issues for intrinsic dielectric constants

Polarization and intrinsic dielectric constant cannot be directly measured for samples. Instead, they are measured via the electric current [I(t)] in the measurement circuit. For D-E loop tests using the modified Sawyer-Tower circuit, integration of I(t) yields the electric displacement,

D(t).[68] For BDS measurements, the complex capacitance (C_p^*) is obtained via the complex I(t)*:[69]

$$C_p^* = -i\frac{I(t)^*}{\omega V(t)} \quad (6)$$

where ω is the angular frequency (ω = 2π*f*, where *f* is frequency) and V(t) is the applied sinusoidal voltage. From the above discussion, interfacial polarization from space charges (i.e., impurity ions and electrons) and charge injection into the conductive pathways in direct contact with metal electrodes can substantially increase the apparent C_p^* measured for the sample. In addition, stray capacitance (C_{str}, i.e., parasitic capacitance from the test circuit) is also present, and its imaginary part should equal to zero. When the sample capacitance (C^*_{sam}) decreases to a value comparable to C_{str}, a large error in the measured dielectric constant is resulted. This often happens for thick (e.g., >100 μm) film samples with a low dielectric constant. Considering all these factors, the measured C_p^* is:

$$C_p^* = C^*_{sam} + C^*_{ion} + C^*_{elect} + C^*_{inj} + C_{str} \quad (7)$$

where C^*_{ion} and C^*_{elect} are capacitance from conduction of ions and electrons (i.e., hetero-charges), and C^*_{inj} is the capacitance from injected homo-charges via the conduction pathways. If we use the following equation, the calculated dielectric constant ε_r^* will be significantly overestimated:

$$C_p^* = \varepsilon_r^* \varepsilon_0 (A/d) \quad (8)$$

where A is the area and d is the thickness of the film sample.

To accurately measure C^*_{sam}, we need to i) avoid C^*_{inj}, ii) subtract C_{str}, and iii) subtract C^*_{elect}. C^*_{inj} can be avoided by uniformly dispersing conductive fillers in the polymer matrix. If carbon nanotubes are embedded in a polymer matrix, C^*_{inj} is somewhat difficult to avoid because of its good conductivity and high aspect ratios. For Novocontrol Concept 80, C_{str} is about 0.6-1.0 pF when the sample is put in the shielding chamber. If the sample is thick (e.g., >100 μm),

area is small (diameter <3 mm), and dielectric constant is low (e.g., <3), C_{str} becomes comparable to C^*_{sam}. As such, it should be subtracted. Note that C^*_{elect} has only the imaginary part and no real part ($C'_{elect} = 0$), because electrons can go through the metal electrodes and will not store any energy. The $\varepsilon''_{r,elect}$ is calculated by $\varepsilon''_{r,elect} = \sigma_e/(\omega\varepsilon_0)$, where the electronic conductivity (σ_e) is measured by the leakage current test. It should be subtracted from the $\varepsilon_r''(\omega)$. Finally, C^*_{ion} has both real and imaginary parts, because the metal electrodes serve as blocking electrodes.[70, 71] It can be extremely large compared to C^*_{sam}. Even a ppm level of impurity ions can cause very large C^*_{ion}, especially at low frequencies ($<10^3$ Hz) because of the slow motion of ions. In principle, C^*_{ion} can be subtracted using the Havriliak-Negami (HN) deconvolution method.[72] However, it is not particularly easy. If C^*_{ion} exists in the sample, one should be cautious not to claim the measured large value of apparent ε_r' (usually $>10^3$) as the intrinsic dielectric constant.

With accurate dielectric measurements, the intrinsic dielectric constants based on electronic, atomic, and orientational polarizations for organic polymers generally should not exceed ~200. Note that the dielectric constant for water at room temperature is about 80.[73] The dielectric constant for N-methylformamide is about 180 at room temperature, which is considered to be the highest for organic molecules.[74] If the measured apparent ε_r is beyond ~200, one should carefully examine what could be the reason, C^*_{inj} or C^*_{ion}.

3.2. Limited dielectric constant from electronic and atomic polarizations

Among all contributions to the intrinsic dielectric constant, electronic and atomic polarizations are the most desired, because the related dielectric loss mechanisms happen above the infrared frequencies and there is no dielectric loss in the power and radio frequency ranges. However, for hydrocarbon-based organic polymers, their contributions are quite limited. As

shown in Fig. 5, the dielectric constants from electronic and vibrational polarizations are calculated for hundreds of polymers using density functional theory (DFT).[75] An upper limit boundary relationship as a function of band gap is observed for the electronic dielectric constant (Fig. 5a). If we consider the band gap for insulating polymers is 4 eV, the upper limit electronic dielectric constant is about 4.0. Atomic (or ionic for ceramic crystals) dielectric constant ranges from 10% to 35% of electronic dielectric constant, and it does not have a well-defined relationship with band gap (Fig. 5b). Adding both together, the upper limit dielectric constant is about 5.0 for insulating polymers with band gap > 4 eV (Fig. 5c). Therefore, many common polymers exhibit a relatively low $\varepsilon_{r\infty}$ below 5.0.

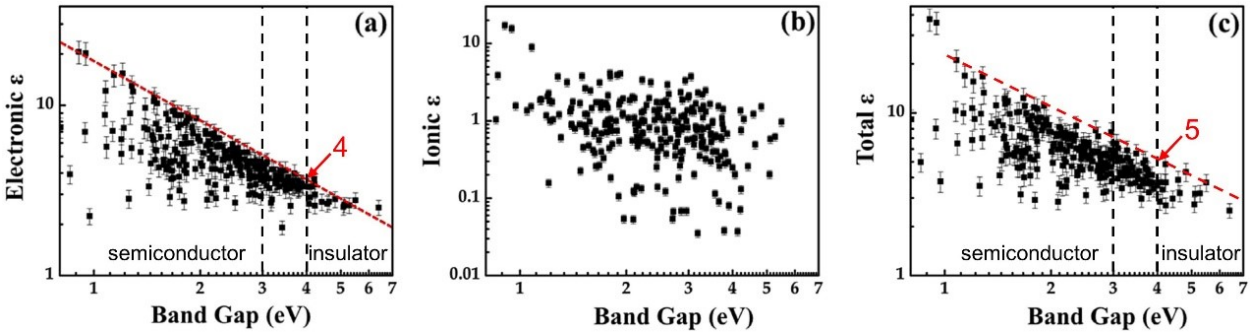

Fig. 5. (a) Electronic, (b) atomic (or ionic), and (c) total dielectric constant, $\varepsilon_{r\infty}$, as a function of the band gap for hydrocarbon-based polymers, computed using density functional theory (DFT) within the single chain approach.[73] Copyright 2014. Reproduced with permission from Elsevier Science Ltd.

Practically, electronic polarization can be enhanced by delocalizing electrons in conjugated π orbitals. For example, conjugated polymers such as poly(3-hexyl thiophene) (P3HT) have a higher dielectric constant (ca. 3.5-4) than BOPP.[76] However, polymers with long conjugation lengths are semiconducting (band gap < 3 eV), and have a high conductivity because of the presence of space charges (either electrons or holes). Meanwhile, semiconducting polymers can be easily doped to exhibit metallic conductivities. Therefore, they are not suitable for high-

voltage electric energy storage. If the conjugation length is rather short (e.g., a few repeat units), an enhanced electronic dielectric constant can be obtained without the semiconducting property. For example, polymers grafted with conjugated fluorescein side groups are reported to exhibit relatively high $\varepsilon_{r\infty}$ between 4 and 6.[77] Nevertheless, the enhancement is still rather limited.

Based on the theory of electrostatics,[14] vibrational polarization can be enhanced by replacing carbon atoms in organic polymers with larger atoms, such as Si and Ge. This is further confirmed by recent DFT simulation.[75] However, dielectric constants for Si-based polymers such as polydimethylsiloxane are not high (only ~2.8),[78] and Ge-based polymers rarely exist. Later, Sn and Zn-containing polymers are proposed.[20] Nevertheless, there is a concern that organometallic polymers may have a low band gap, and can be easily contaminated with impurity ions. The other way to enhance atomic polarization is to increase the polarity for polymers, because polar vibrational modes in the infrared frequencies create large induced dipoles. For example, crystalline cellulose and amino acids/proteins exhibit relatively high dielectric constants of 6-7.[79, 80] Recently, aromatic polythioureas (ArPTUs) are also found to show relatively high dielectric constant between 4 and 6 with high energy density and relatively low loss.[81-84] However, highly polar polymers are easy to absorb moisture, which is detrimental to dielectric insulation. Therefore, it is desired to encapsulate polar polymers for capacitor applications. Later, we will introduce the multilayer film technology to tackle this problem.

Finally, it is worth mentioning a high dielectric constant copper phthalocyanine (CuPc)[85, 86] and its related polymers.[87-91] The CuPc is synthesized from pyromellitic anhydride or 1,2,4,5-tetracyanobenzene either in solution or in melt.[92, 93] Because of the one-pot reaction, multiple components are obtained as the final product, including (either linear or fused cyclic) oligomers and monomers. The periphery carboxylic acid groups make the CuPc insoluble in

most solvents (only the sodium carboxylate form is soluble in water), rendering molecular characterization difficult. Nonetheless, a tetrameric cyclic form was assumed in the early publications.[92, 93] Using BDS study, the conjugated CuPc is found to show a very high dielectric constant (>10^5) with a high electronic polarizability of 1.2×10^{-22} cm^3.[85, 86, 94] Later, the CuPc is either blended with or grafted onto polymers using the periphery carboxylic acid groups.[87-91] Again, high dielectric constants of a few hundreds are reported, and electroactive actuation is proposed for these high dielectric constant polymers. However, it is recently proved that the CuPc is not the cyclic tetramer, but the monomer (~30%) with a trace amount of dimers (2-3%).[95-97] The ultrahigh dielectric constant at low frequencies should be attributed to absorbed water and subsequent ionization of the carboxylic acid groups (i.e., proton conductivity).[95, 98] At low relative humidity and high frequencies, the dielectric constant of CuPc is only about 10 as measured by BDS.

For $\varepsilon_{r\infty}$, the measurement should be conducted in the optical/infrared frequencies. However, this is not possible for non-transparent and infrared-absorbing samples such as CuPc. When BDS is used, one had better use the ε_r' data at low temperatures (e.g., -150 °C) and high frequencies (e.g., 1 MHz). Under this condition, most space charge and orientational polarizations are prohibited, and the ε_r' value should be close to the $\varepsilon_{r\infty}$. Otherwise, high apparent dielectric constants will be reported for polymers containing conjugated oligomeric groups.[99]

3.3. Enhancing dielectric constant using orientational polarization

As mentioned above, pure water has a high dielectric constant of ~80 at room temperature.[73] Its dipolar relaxation happens around 10 GHz, and thus its dielectric loss is low (e.g., tanδ ~ 0.005) in the power frequency range (10^3-10^6 Hz). Despite the unknown structure

for water, it is speculated that polar nanoregions due to directional hydrogen-bonding are responsible for its high dielectric constant.[100] Learning from water, it is desired to achieve high dielectric constant via orientational polarization for polymers.[18]

3.3.1. Normal ferroelectric polymers

During the past a few decades, PVDF and its random copolymer films were ever attractive for film capacitors. This is because they exhibit a relatively high dielectric constant ($\varepsilon_r \sim 10$) at room temperature, which could be attributed to the high dielectric constant amorphous phase above the glass transition temperature ($T_g \sim -40$ °C).[101] Note that linear dielectric constants are often measured using BDS under a very low electric field (<0.2 MV/m). Under such a low field, PVDF crystals do not contribute to the orientational polarization. However, as the electric field increases to above the coercive field (E_c = 70-120 MV/m, depending on the α and β contents), PVDF crystals become ferroelectric with broad hysteresis loops, regardless of which crystalline form they are in (totally, there are five crystalline forms: nonpolar α and ε, and polar β, γ, and δ).[102, 103] Among all crystalline forms, the β form with an all trans planar chain conformation possesses the largest spontaneous polarization (P_s), ~185 mC/m^2, as calculated by DFT.[104] This large P_s is about 1.5 times that (~130 mC/m^2) of the rigid dipole model calculated by MD simulation.[105] The ~50% increase in P_s is attributed to additional electronic polarization induced by the dipole-dipole coupling interaction, when all trans planar PVDF chains are tightly packed in the β crystalline lattice.

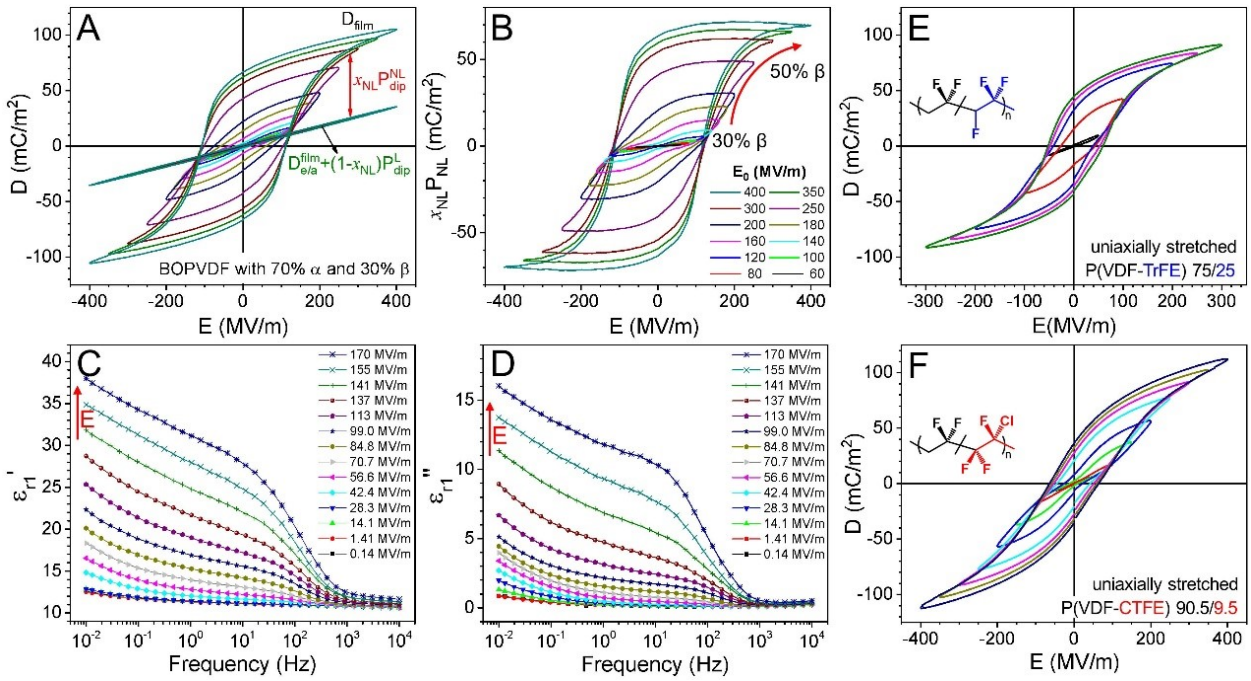

Fig. 6. (A) Progressive bipolar D-E loops for a commercial BOPVDF film containing 70% α and 30% β phases. By subtracting the linear dielectric contribution, the nonlinear dielectric response is shown in (B). Upon poling to 400 MV/m, the β content gradually increases to ca. 50%. (C) and (D) show the linear dielectric constants, ε_{r1}' and ε_{r1}'' as a function of frequency under different poling fields at 25 °C.[67] Copyright 2016. Adopted with permission from American Chemical Society. (E) Bipolar D-E loops for a uniaxially stretched P(VDF-TrFE) 75/25 film (500% stretching ratio). The film was polarized at 200 MV/m first. (F) Bipolar D-E loops for a uniaxially stretched P(VDF-CTFE) 90.5/9.5 film (500% stretching ratio).[114] Copyright 2017. Adopted with permission from American Chemical Society. All D-E loops use a poling frequency of 10 Hz with a sinusoidal waveform.

Fig. 6A shows progressive bipolar D-E loops (10 Hz) for a commercial (Kureha) biaxially oriented PVDF (BOPVDF) film containing 70% α and 30% β phases.[69, 101] During high field poling, the nonpolar α phase undergoes an irreversible phase transition into the polar δ phase around 100-130 MV/m.[106, 107] Above 200 MV/m, the δ phase will gradually transform into the γ and ultimately the β phase. At the end of 400 MV/m bipolar poling, the β phase content increases to ca. 50%. Note that these electric field-induced phase transformations are not reversible. After subtracting the linear dielectric contribution from electronic/atomic polarizations ($D_{e/a}^{film}$) and orientational polarization of the linear amorphous phase [(1-x_{NL})P_{dip}^{L}],

the nonlinear dielectric component ($x_{NL}P_{dip}^{NL}$) can be obtained:

$$x_{NL}P_{dip}^{NL} = D_{film} - \left[D_{e/a}^{film} + (1 - x_{NL})P_{dip}^{L}\right] \quad (9)$$

where x_{NL} is content of the nonlinear component (e.g., crystalline δ, γ, and β phases) and D_{film} is electric displacement of the film. From the linear dielectric contribution [$D_{e/a}^{film} + (1 - x_{NL})P_{dip}^{L}$], the apparent linear dielectric constant is calculated to be ~10, which is beneficial for electric energy storage. However, the nonlinear dielectric response in Fig. 6B is undesired, because all nonlinear components contribute to energy losses. This is exactly reflected by the high-voltage BDS results of linear dielectric constants, ε_{r1}' and ε_{r1}'', in Figs. 6C and D.[69] As the poling field increases above the E_c, significant dielectric loss is observed. Moreover, ferroelectric switching stops around 1000 Hz, because ferroelectric domains are too large to be switched quickly.

It is highly desired to minimize or even eliminate the nonlinear ferroelectric switching in PVDF for film capacitors.[18, 103] However, it is not a trivial task. One approach is to decrease the domain sizes into the nanometer scale (i.e., nanodomains) to ease ferroelectric switching. For example, it has been reported that relaxor ferroelectric ceramics have a disordered organization of 1-3 nm ferroelectric domains in the paraelectric matrix.[108-110] Decreasing the domain sizes for PVDF has been attempted. Since it is difficult to achieve nanodomains in neat PVDF, copolymers with trifluoroethylene (TrFE), chlorotrifluoroethylene (CTFE), and hexafluoropropylene (HFP) are proposed. TrFE has a similar size as VDF. Therefore, TrFE units can be easily included in the PVDF crystal to form repeat unit isomorphism.[111-113] The significant effect of isomorphism is the dramatic decrease of the Curie temperature (T_C) below the melting temperature (T_m) at ambient pressure.[114, 115] Nonetheless, TrFE units cannot break the large ferroelectric domains into nanodomains; instead, they participate in the ferroelectric

domain formation. Fig. 6E shows the bipolar D-E loops for a uniaxially stretched P(VDF-TrFE) 75/25 (mol./mol.) film with a stretching ratio of 500% at room temperature. Although the D-E loops are slimmer than those for BOPVDF in Fig. 6A, significant ferroelectric switching is still observed.

CTFE and HFP units are too large to be included in the PVDF crystal under normal crystallization condition. However, they can disrupt/decrease the crystallite size, which in turn can regulate the ferroelectric domain size, especially in stretched films. Fig. 6F shows the bipolar D-E loops for a uniaxially stretched P(VDF-CTFE) 90.5/9.5 (mol./mol.) film with 500% stretching ratio.[116] From XRD analysis, the crystallite size is only 6 nm. However, the D-E loops still appear to be too broad. Although large discharged energy densities have been reported for P(VDF-CTFE)[117, 118] and P(VDF-HFP)[119] random copolymers, the significant hysteresis loop loss prevents them from being used as practical capacitor films.

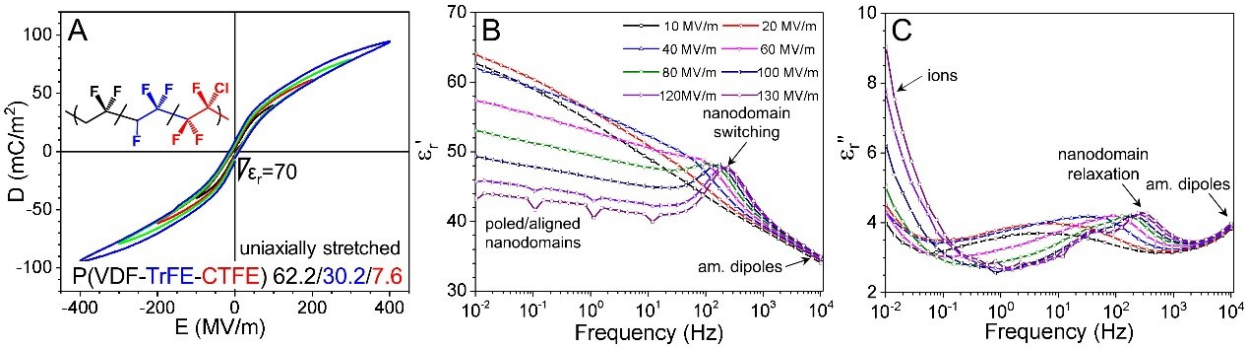

Fig. 7. (A) Bipolar D-E loops for a uniaxially stretched P(VDF-TrFE-CTFE) 62.2/30.2/7.6 (molar ratio) film (stretching ratio = 500%). The poling frequency is 10 Hz.[125] Copyright 2016. Adopted with permission from American Chemical Society. (B) and (C) show high-voltage BDS results of ε_r' and ε_r'' as a function of frequency for the uniaxially stretched P(VDF-TrFE-CTFE) 62.2/30.2/7.6 film at 25 °C. The electric field varies from 10 to 130 MV/m.

3.3.2. Relaxor ferroelectric polymers

Genuine relaxor ferroelectric polymers were first achieved for electron-beam or gamma

ray irradiated P(VDF-TrFE) random copolymers,[120, 121] and large electrostriction was reported.[121, 122] Later, large termonomers, such as chlorofluoroethylene (CFE) and CTFE, are incorporated into P(VDF-TrFE) to synthesize terpolymers.[123-126] Slim D-E loops due to the formation of nanodomains are obtained. Weak physical pinning of CFE units in the P(VDF-TrFE) crystal leads to double hysteresis loops,[113] whereas strong physical pinning of CTFE units results in narrow single hysteresis loops (Fig. 7A).[127, 128] The apparent dielectric constant for P(VDF-TrFE-CTFE) reaches ~70, close to that of water, at room temperature. Figs. 7B and C show high-voltage BDS results of ε_r' and ε_r'' for this uniaxially stretched P(VDF-TrFE-CTFE) film. Upon increasing the electric field to above 60 MV/m, dielectric constant below 10 Hz gradually decreases. This is ascribed to the formation of aligned ferroelectric domains when the electric field is high and the frequency is low. As the frequency increases to around 300 Hz, there is no time for the ferroelectric domain to stay aligned. As a result, a peak appears in ε_r' when the field is beyond 80 MV/m (Fig. 7B). Meanwhile, a relaxation peak for the nanodomains is observed in ε_r'' (Fig. 7C). Beyond 3000 Hz, ferroelectric switching of nanodomains stops, and the amorphous dipole relaxation is observed above 10^4 Hz.

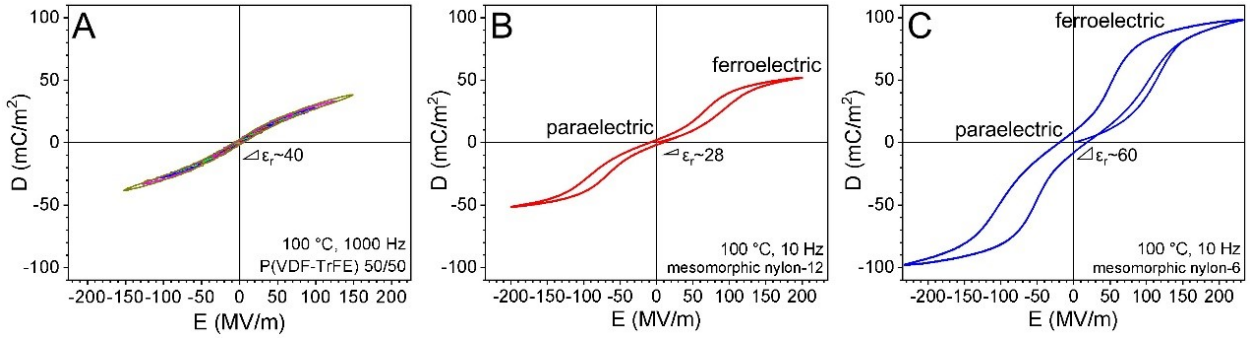

Fig. 8. Bipolar D-E loops for uniaxially stretched (A) P(VDF-TrFE) 50/50 ([127] Copyright 2012. Adopted with permission from Elsevier Science Ltd.) and bipolar D-E loops for uniaxially stretched (B) mesomorphic nylon-12, and (C) mesomorphic nylon-6 films.[128] Copyright 2017. Reproduced with permission from American Chemical Society. For mesomorphic nylon-12 and nylon-6 films, AC electronic conduction is subtracted.

3.3.3. Paraelectric polymers

Although a high dielectric constant of 70 has been achieved for the relaxor ferroelectric P(VDF-TrFE-CTFE) terpolymer, the dissipation factor is relatively high; tanδ = 0.08 as calculated from Figs. 7B and C. This is attributed to the presence of ferroelectric nanodomains. Meanwhile, the dielectric constant will be low for high fields and high frequencies, because nanodomains stop switching under these conditions. In this sense, paraelectric polymers could be a better choice. Two types of paraelectric polymers exist for polymers. The first is a molten polar polymer melt, where molecular dipoles can easily rotate. However, polymer melts are not suitable for film capacitors because of significantly enhanced ionic and electronic conduction. The second is a paraelectric semicrystalline polymer. Because of the enlarged interchain distance in the crystals, polymer chains and dipoles can also easily rotate.[106] As shown in Fig. 8A, a uniaxially stretched P(VDF-TrFE) 50/50 film exhibits narrow single hysteresis loops with a relatively high apparent dielectric constant of ~40.[129] This is because no ferroelectric domains could form during the high-field electric poling. If transient (or metastable) ferroelectric domains can form at a high enough poling field, double hysteresis loops will be obtained as a result of reversible paraelectric-to-ferroelectric transitions. This is observed for mesomorphic nylon-12 (Fig. 8B) and nylon-6 (Fig. 8C) at 100 °C, respectively.[130] The apparent dielectric constants for mesomorphic nylon-12 and nylon-6 are 28 and 60, respectively. The disadvantage of paraelectric polymers is their high electronic conductivity because of the highly mobile amorphous and crystalline phases.

3.3.4. Dipolar glass polymers with reduced dielectric losses

As we can see from the above discussion, large-scale molecular motions in polar polymers is easy to promote cooperative dipolar activities (i.e., formation of ferroelectric domains) and ionic/electronic conduction. To tackle this problems, we propose dipolar glass polymers (DGPs), where the chain motion is largely frozen (e.g., in the glassy state) and only dipolar groups can rotate locally (i.e., sub-T_g transitions) to increase dielectric constant.[131] Depending on the location of dipolar groups, DGPs can be divided into two categories: main-chain and side-chain DGPs. Examples of the main-chain DGPs include aromatic polyimides (PI),[132-134] polyamides,[135] and polythiourea.[81-84] First, polar PIs with cyano groups directly attached to the phenyl rings in the main chain exhibited dielectric constants around 3.75 at room temperature.[132] Yang et al. introduced crown ether groups into PI backbone and synthesized a series of PI with a high dielectric constant (5.8-6.4) and low loss ($\tan\delta < 0.02$) at the frequency range of 100-100,000 Hz.[134] Second, aromatic polyamides include both semi-aromatic and fully aromatic polymers. Semi-aromatic polyamides are Selar (DuPont) and MXD series (Mitsubishi). Their dielectric constants are around 5.[135] Fully aromatic polyamides include Kevlar and Nomex; however, they are difficult to be processed into high quality thin films for capacitor applications. As we mentioned above, ArPTUs exhibit a relatively high dielectric constant of 4.5-6 due to the high dipole moment of the thiourea unit (4.89 D), and $\tan\delta$ is lower than 0.01 between 100 and 1 MHz.[81] The discharged energy density at 1 GV/m is as high as 22 J/cm^3 with an efficiency of 92.5%. Note, it is difficult to clearly differentiate high-frequency orientational polarization from vibrational polarization, when the rotation of polar groups is vibration-like.

As we can see, the rotation of dipolar groups in the main chain is rather limited. To

enhance the orientational polarization and thus dielectric constant for DGPs, the polar groups should be attached in the side chains. Side-chain DGPs can be either glassy or semicrystalline. Common dipolar groups include hydroxyl (-OH, 1.7 D), carbonyl (-C=O, 2.3 D), cyano (-CN, 3.7 D), and sulfonyl ($-SO_2CH_3$, 4.5 D) groups. When hydroxyl groups are introduced into the pendant group of polypropylene (PP-OH), the dielectric constant becomes twice that of PP, and increases proportionally with the -OH content. For example, the dielectric constant of PP-OH with 4.2 mol.% of the OH comonomer reaches 4.6.[136] The dielectric loss of PP-OH is reasonably low. It is known that regenerated celluloses (only 30-40% crystallinity) exhibit dielectric constant as high as 7-10.[137, 138] Again, this is attributed to the orientational polarization of the $-CH_2OH$ side groups in the glassy amorphous phase.

Cyanoethyl ($-CH_2CH_2CN$) or cyanomethyl ($-CH_2CN$) side groups are also used for side chain DGPs. When $-CH_2CN$ groups are attached as the side chains in a bisphenol A polycarbonate (i.e., CN-PC), the dielectric constant at 1 kHz increases to 4.0 for CN-PC as compared to that of 2.9 for neat PC.[139] The dissipation factor is reasonably low, i.e., $\tan\delta \sim 0.005$ at 130 °C and 1 kHz. However, the dielectric constant is low due to the low density of the $-CH_2CN$ dipoles. Cyanoethylated poly(vinyl alcohol) (CN-PVA) exhibits a dielectric constant of ca. 10 and a minimum $\tan\delta$ of 0.01 at 1 Hz below its T_g of 25 °C.[140] Cyanoethylated poly(2,3-dihydroxylpropyl methacrylate) (CN-PDPMA) has a relatively high dielectric constant (ca. 8) between the β (rotation of $-CH_2CH_2CN$ dipoles at -60 °C) and the α (T_g at 25 °C) transitions at 500 Hz.[141] However, the window between the β and α transitions is narrow, only about 85 °C. Also, the T_gs for CN-PVA and CN-PDPMA (and some cyanoethylated celluloses[142]) are too low for applications above room temperature. The low T_g of cyano-ethylated polymers can be attributed to the relatively long side chains. To overcome this problem, Shin-Etsu Chemical

commercialized cyanoethylated pullulan (CEP, ~90% functionality). Because of the rigid cellulose backbone structure, the T_g reaches ca. 110 °C,[143] and the dielectric constant at room temperature is around 16 at 10^4 Hz. Despite these attractive dielectric properties, CEP suffers from relatively low T_g, low dielectric breakdown strength (ca. 100 MV/m), and insufficient dipole switching speed (<10^4 Hz).

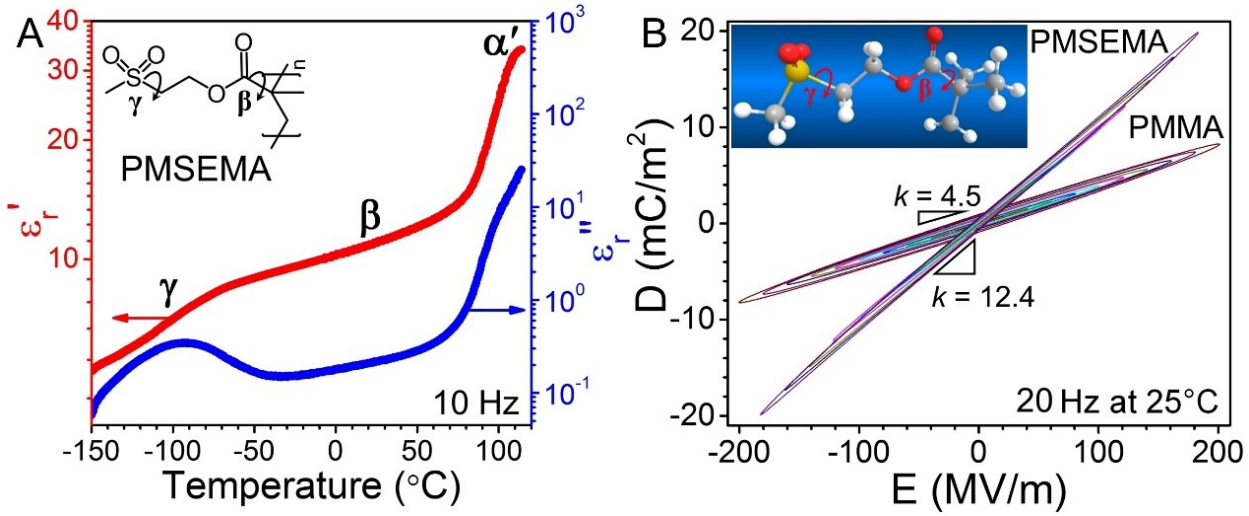

Fig. 9. (A) Temperature-scan BDS results of ε_r' and ε_r'' at 10 Hz for PMSEMA. (B) Bipolar D-E loops for PMSEMA in comparison with those for PMMA.[142] Copyright 2015. Reproduced with permission from American Chemical Society.

Finally, sulfonyl groups are also incorporated into the side chain DGPs to enhance dielectric constant.[144, 145] Poly[2-(methylsulfonyl)ethyl methacrylate] (PMSEMA) is prepared by introduced methylsulfonyl group through flexible ether group.[144] Fig. 9A shows that PMSEMA shows an obvious γ transition at -100 °C at 10 Hz and T_g around 109 °C due to the large dipole moment of small sized sulfonyl groups. PMSEMA exhibits a high dielectric constant of 11-12 and a reasonable dielectric loss of 0.02 at 25 °C. At room temperature, PMSEMA exhibits linear D-E loops with apparent dielectric constant nearly 3 times that of PMMA, an analogue polymer (Fig. 9B).

Similar enhancement in dielectric constant is also found in sulfonylated polyepichlorohydrin (PECH) and poly[3,3-bis(chloromethyl)oxetane] (PBCMO) with one and two methylsulfonyl groups per repeat unit, respectively.[146] The disulfonylated DGPs show higher dielectric constants (ε_r = 9-12) than the monosulfonylated DGPs (ε_r = 7-8). However, disulfonylated DGPs have higher dielectric losses than the monosulfonylated DGPs. Due to the aliphatic nature, these polyether-based DGPs have relatively low T_g values (i.e., <125 °C).

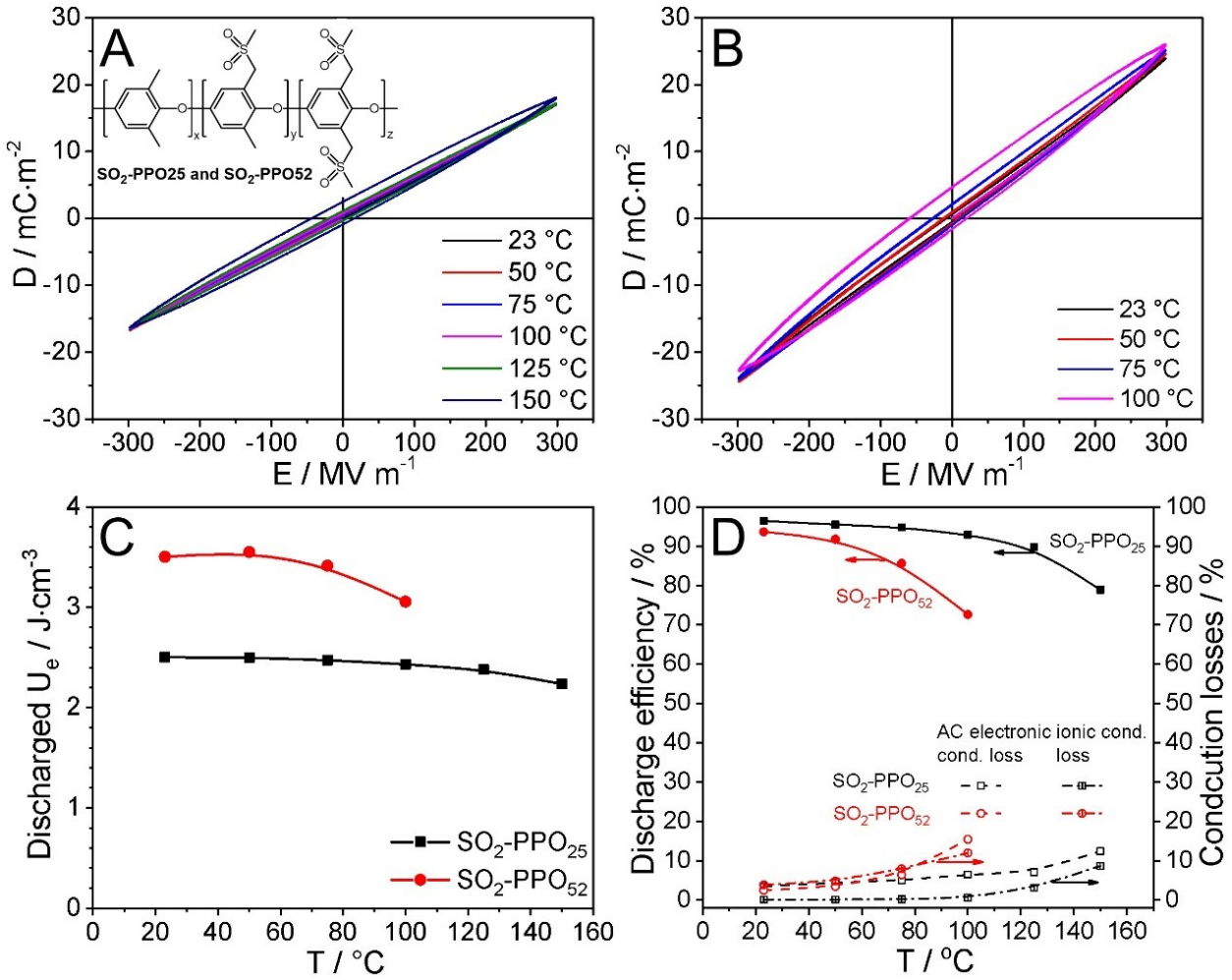

Fig. 10. Bipolar D-E loops at different temperatures for (A) SO_2-PPO_{25} and (B) SO_2-PPO_{52}. The inset in (A) shows the chemical structure of the sulfonylated PPO. (C) Discharge energy densities (U_e) and (D) discharge efficiencies as a function of temperature for SO_2-PPO_{25} and SO_2-PPO_{52}.[145] Copyright 2018. Adopted with permission from John Wiley & Sons Inc.

To further enhance heat resistance, sulfonylated poly(2,6-dimethyl-1,4-phenylene oxide) (SO_2-PPO) is synthesized via post-polymer functionalization (see inset of Fig. 10A).[147] The rigid backbone of PPO not only improves the T_g (~220 °C) but also provides enough free volume for the efficient rotation of methylsulfonyl groups below T_g. Therefore, the dielectric constant and discharge energy density of SO_2-PPO can reach as high as 8.8 and 24 J/cm^3, respectively, at room temperature. The dissipation factor is as low as 0.003. Temperature dependent D-E loops for SO_2-PPO_{25} and SO_2-PPO_{52} are shown in Figs. 10A and B, respectively. Narrow loops are observed. The discharge energy densities (U_e) and discharge efficiencies are seen in Figs. 10C and D, respectively. It is seen that SO_2-PPO_{25} has a lower U_e; however, its discharge efficiency is much higher at high temperatures. The loss mechanism is attributed to both electronic (major) and ionic (minor) conduction at high temperatures (Fig. 10D). Therefore, rigid backbone and appropriate dipole density are important for the high temperature film capacitor application.

Most recently, a new class of dipolar glass polymers was synthesized based on an organo-soluble polymer of intrinsic microporosity (PIM) bearing sulfonyl side groups.[148] Again, as a result of orientational polarization of the sulfonyl side groups, relatively high dielectric constant ~6 is achieved. The discharged energy density is as high as 17 J/cm^3 around 800 MV/m. This dipolar glass PIM is used, together with the silica layer (230 nm), as the gate dielectric on highly doped silicon for InSe field effect transistors. About 10× increased electronic mobility is achieved as compared to the neat silica dielectric layer. This opens a new opportunity for high κ polymers to be used as gate dielectrics in FETs.

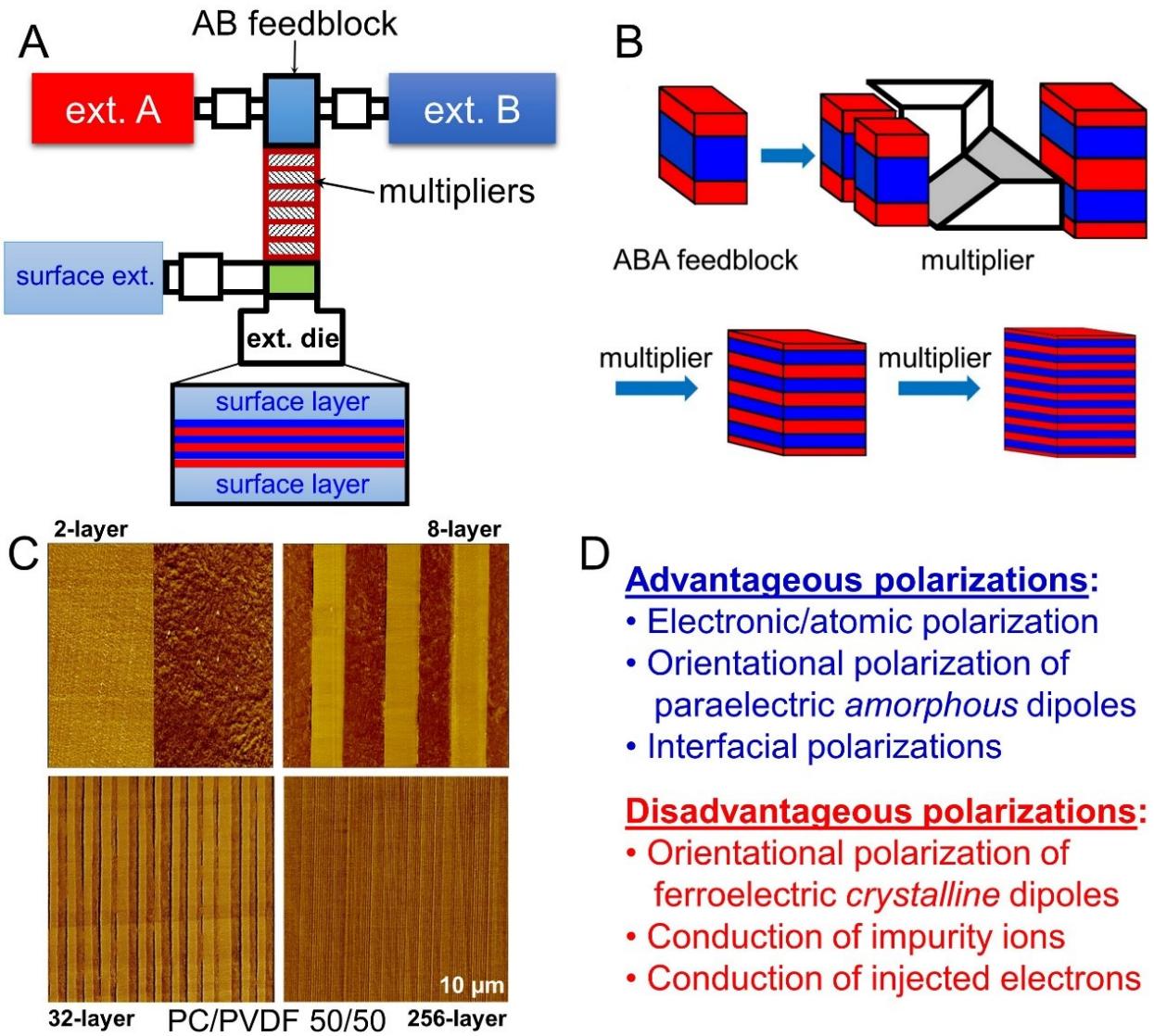

Fig. 11. Schematic representations of (A) the multilayer coextrusion line and (B) the layer multiplication process. (C) AFM images of PC/PVDF 50/50 (vol./vol.) 2-, 8-, 32-, and 256-layer films. (D) Summary of advantageous and disadvantageous polarizations in multilayer films.[4] Copyright 2017. Adopted with permission from American Chemical Society.

4. Combined intrinsic and extrinsic polymer dielectrics: Multilayer films

From the above discussion, polarization and dielectric constant can be enhanced via orientational polarization. Therefore, polar polymers bearing dipolar groups should be the future direction for high temperature, high energy density, and low loss dielectrics. However, there are still some concerns for highly polar polymers. First, polar polymers are easy to absorb moisture,

which is detrimental for electric insulation. Second, polar polymers are easy to be contaminated with impurity ions, and ionic conduction can induce high dielectric loss, especially at high temperatures. Third, like water, highly polar polymers can form nonionic EDL when they are in direct contact with metal electrodes. The large voltage drop (or high local field) in the thin EDL will induce electrochemical reactions. Indeed, electrochemical degradation of PVDF and nylons has been reported previously at elevated temperatures under high electric fields.[149, 150] To mitigate these potential problems, we have proposed multilayer polymer films.[4] In these films, a high dielectric constant polar polymer (e.g., PVDF and nylons) is multilayered with a high breakdown strength/low loss linear dielectric polymer [e.g., PC, polysulfone, and poly(ethylene terephthalate (PET)], using the multilayer coextrusion technology.[151] Schemes of the coextrusion line and multiplication processes are shown in Figs. 11A and B, respectively.[152] By matching the melt viscosities of the two polymers, multilayer films with different numbers of layers can be obtained. Fig. 11C shows atomic force microscopy (AFM) phase images of the polished cross-sections of PC/PVDF 50/50 (vol./vol.) multilayer films with 2-, 8-, 32-, and 256-layers.

These multilayer films actually combine intrinsic and extrinsic dielectric properties together, among which some are advantageous and some are disadvantageous (Fig. 11D). The research goal is to enhance the advantageous polarizations and minimize the disadvantageous polarizations. The advantageous polarizations include electronic/atomic polarizations, linear orientational polarization of paraelectric amorphous dipoles in PVDF (or nylons), and dipolar and space charge interfacial polarizations (see Fig. 1). The disadvantageous polarizations include nonlinear orientational polarization of ferroelectric crystalline domains in PVDF (or nylons), conduction of impurity ions, and conduction of injected electrons from metal electrodes. Below,

we use PVDF-based multilayer films to illustrate the above considerations.

These multilayer films exhibit enhanced dielectric constant between 4 and 7, which can be adjusted by tuning the PVDF volume fraction (see Eqn. 2 and Fig. 2B). In these multilayer films, both dipolar and space charge interfacial polarizations exist, as a result of large dielectric constant and conductivity contrasts (Fig. 1). These interfacial charges (σ_{dip} and σ_{sp}) can serve as effective blocks to prevent the passage of injected hot electrons from the cathode through the film.[153, 154] Indeed, dielectric breakdown strengths are enhanced for the multilayer films, when compared to the linear addition line of breakdown strengths of the individual component polymers.[4, 37, 155]

Multilayer film is the optimal approach to mitigate ferroelectric switching in PVDF.[22] Because of the nonuniform electric field distribution, the high dielectric constant PVDF layers bear a significantly lower local field than the applied electric field. Consequently, ferroelectric switching is effectively prevented if the external field is not too high. Multilayer films also provide a confined environment for the impurity ion conduction. As the PVDF layer thickness gradually decreases, the conduction of impurity ions is effectively blocked by the neighboring PC layers.[22] Finally, multilayer films with PC as the outer layers can prevent the direct contact of PVDF with metal electrodes and thus easy injection of hot electrons into PVDF. As a result, electronic conduction can be reduced in multilayer films, as compared to that in the polar polymer. Our experiments show that the higher the T_g for the outer linear polymer (PC or PSF), the less charge injection from the metal electrodes.[156] After system optimization for the PC/PVDF multilayer films, we have achieved high energy density at breakdown (13-17 J/cm^3), high breakdown strength (>600 MV/m), high temperature capability (up to 125 °C), and low dissipation factor ($\tan\delta$ = 0.005 at 1 kHz). Currently, we are collaborating with industrial partners to scale up the fabrication of multilayer films, and package and test multilayer film capacitors.[157]

5. Conclusions and outlook

In summary, high energy density and low loss polymer dielectrics are highly desired for electric energy storage applications in the power frequency range (100 to 10^6 Hz). Rich condensed matter physics is involved in the development of next generation dielectric polymeric materials. In order to realize practical applications for new dielectric polymers, the priority should focus on decreasing the dielectric loss while trying to enhance dielectric constant and energy storage. Due to the conflicting nature of low dielectric loss (better to be nonpolar polymers) and high polarization/dielectric constant (better to be polar polymers), we can only achieve a delicate balance between them. Although extrinsic interfacial polarizations in nanodielectrics and ion gels can significantly boost the overall capacitance, reduced dielectric breakdown strength and high conduction losses are resulted. Therefore, enhancing intrinsic dielectric constant from electronic, atomic, and orientational polarizations should be pursued for next generation polymer dielectrics in terms of electric energy storage.[18]

First, it is the most desired to enhance electronic and atomic polarizations, because they are above the terahertz frequency and will not have any loss in the power frequency range. Nonetheless, the molecular bonding nature of organic polymers prevents significant enhancement of electronic and atomic polarizations without lowering the band gap. Second, orientational polarization has a potential to increase the intrinsic dielectric constant while maintaining a reasonably low dielectric loss. In this sense, polar polymers with highly dipolar groups in the main chain or the side chains are desired. However, nonlinear ferroelectric switching should be avoided, whether normal ferroelectric or relaxor ferroelectric polymers. For linear orientational polarization, paraelectric polymers seem to be promising, because they do not have any

ferroelectric domains. However, the high chain mobility in the paraelectric phase often facilitates high electronic conduction. Therefore, dipolar glass polymers are more promising, because chain dynamics is largely frozen to prevent conduction of charge carriers. For side-chain dipolar glass polymers, localized rotation of molecular dipoles in the free volume (i.e., sub-T_g transitions) enhances the dielectric constant. Alternatively, main-chain dipolar glass polymers can be attractive, and small-amplitude vibration rather than large-angle rotation of molecular dipoles is responsible for the enhanced dielectric constant.

To prevent potential moisture absorption for polar polymers, it is possible to combine nonpolar and polar polymers into multilayer films, where extrinsic and intrinsic dielectric properties can cooperate synergistically. With the proper design of the multilayer film architecture, dipolar and space charge interfacial polarizations can become advantageous. For example, dipolar and space charge interfacial polarizations can be utilized to enhance dielectric breakdown strength, because interfacial charges can serve as effective barriers for the conduction of injected hot electrons (see Fig. 1). Meanwhile, confined transport of impurity ions in multilayer films can also reduce the conduction loss from impurity ions. Therefore, multilayer films are promising to become next generation high energy density, high temperature, and low loss polymer dielectrics for electric energy storage applications.[4]

Nevertheless, this review cannot cover all the aspects for next generation polymer film capacitors. We just briefly discuss them below. First, charge (or hot electron) injection from metal electrodes (through either Schottky or Fowler-Nordheim field electron emissions[14, 158]) is serious at high temperatures. How to mitigate charge injection for high temperature polymers is a future research direction.[11, 12] Second, electronic, thermal, electromechanical, and partial discharge breakdowns have been identified for dielectric films.[159] However, their

fundamental mechanisms are not well-understood in terms of both chemical reactions and physical changes. Future research should focus on understanding various breakdown mechanisms and their interactions. Third, self-healing is a fundamental requirement for polymer film capacitors to exhibit a long lifetime.[160, 161] It allows for the use of polymer films that have some intrinsic defects as manufactured. When electric current starts to flow through a defect site as a precursor to breakdown, the local thin metallization is vaporized, thus removing the defect much like a fuse. At this moment, the self-healing mechanism is still unclear. Very few polymers can self-heal successfully except for BOPP. The self-healing mechanism can be optimized by the selection of the metallization material and thickness, and must be able to precede catastrophic faults at elevated temperatures under high voltage stresses. Future research is needed to understand the fundamental mechanism of self-healing and realize it for high temperature polymers. Fourth, advanced film processing needs be developed to achieve the ultimate film thickness of 2-3 μm in order to compete with current BOPP technology in terms of material costs. Other than a handful of high temperature polymers such as PET and PEN,[13] biaxial orientation of other high temperature polymers using the tenter-line technology is rather limited. Once a viable candidate is identified (e.g., the multilayer films), biaxial orientation should be developed at the industrial scale using the tenter-line technology.

Acknowledgements

JW acknowledge financial support from National Nature Science Foundation of China (NSFC, No. 51903016) and Shaanxi Provincial Natural Science for Basic Research (No. 2019JQ-684). LZ acknowledges financial support from the Polymers Program, Division of Materials Research (DMR) of National Science Foundation (DMR-1708990). The authors thank Dr.

Yanfei Huang for the D-E loops of P(VDF-TrFE) 75/25 and Dr. Yue Li for the high-voltage BDS of the P(VDF-TrFE-CTFE) terpolymer.

References

[1] Sarjeant WJ, Zirnheld J, MacDougall FW. Capacitors. IEEE Trans Plasma Sci. 1998;26:1368-92.

[2] Sarjeant WJ, Clelland IW, Price RA. Capacitive components for power electronics. Proc IEEE. 2001;89:846-55.

[3] Montanari D, Saarinen K, Scagliarini F, Zeidler D, Niskala M, Nender C. Film capacitors for automotive and industrial applications. Proceedings of CARTS U.S.A. 2009; Jacksonville, FL, March 30-April 2, 2009. 11 pp.

[4] Baer E, Zhu L. 50th Anniversary perspective: Dielectric phenomena in polymers and multilayered dielectric films. Macromolecules. 2017;50:2239-56.

[5] Herbert JM. Ceramic dielectrics and capacitors. New York: Gordon and Breach; 1985. 264 pp.

[6] Nishino A. Capacitors: Operating principles, current market and technical trends. J Power Sources. 1996;60:137-47.

[7] Ho J, Jow TR. Characterization of high temperature polymer thin films for power conditioning capacitors. Adelphi, MD: Army Research Laboratory; 2009. 19 pp.

[8] Ho J, Jow TR. High field conduction in biaxially oriented polypropylene at elevated temperature. IEEE Trans Dielectr Electr Insul. 2012;19:990-5.

[9] Sarjeant WJ. Capacitors. IEEE Trans Electr Insul. 1990;25:861-922.

[10] Dreike PL, Fleetwood DM, King DB, Sprauer DC, Zipperian TE. An overview of high-

temperature electronic device technologies and potential applications. IEEE Trans Compon Packag Manuf Technol A. 1994;17:594-609.

[11] Tan D, Zhang L, Chen Q, Irwin P. High-temperature capacitor polymer films. J Electron Mater. 2014;43:4569-75.

[12] Li Q, Yao FZ, Liu Y, Zhang G, Wang H, Wang Q. High-temperature dielectric materials for electrical energy storage. Annu Rev Mater Res. 2018;48:219-43.

[13] Demeuse MT. Biaxial stretching of film principles and applications. Oxford: Woodhead Pub.; 2011. 284 pp.

[14] Kao K-C. Dielectric phenomena in solids: with Emphasis on physical concepts of electronic processes. Boston: Elsevier Academic Press; 2004. 581 pp.

[15] Jow TR, Cygan PJ. Dielectric breakdown of polyvinylidene fluoride and its comparisons with other polymers. J Appl Phys. 1993;73:5147-51.

[16] Liu P, Yen R, Bloembergen N. Dielectric-breakdown threshold, 2-photon absorption, and other optical damage mechanisms in diamond. IEEE J Quantum Electron. 1978;14:574-6.

[17] Sun Y, Bealing C, Boggs S, Ramprasad R. 50+ years of intrinsic breakdown. IEEE Electr Insul Mag. 2013;29:8-15.

[18] Zhu L. Exploring strategies for high dielectric constant and low loss polymer dielectrics. J Phys Chem Lett. 2014;5:3677-87.

[19] Chen Q, Shen Y, Zhang S, Zhang QM. Polymer-based dielectrics with high energy storage density. Annu Rev Mater Res. 2015;45:433-58.

[20] Huan TD, Boggs S, Teyssedre G, Laurent C, Cakmak M, Kumar S, et al. Advanced polymeric dielectrics for high energy density applications. Prog Mater Sci. 2016;83:236-69.

[21] Mackey M, Schuele DE, Zhu L, Baer E. Layer confinement effect on charge migration in polycarbonate/poly(vinylidene fluorid-*co*-hexafluoropropylene) multilayered films. J Appl Phys. 2012;111:113702/1-9.

[22] Mackey M, Schuele DE, Zhu L, Flandin L, Wolak MA, Shirk JS, et al. Reduction of dielectric hysteresis in multilayered films via nanoconfinement. Macromolecules. 2012;45:1954-62.

[23] Yang L, Allahyarov E, Guan F, Zhu L. Crystal orientation and temperature effects on double hysteresis loop behavior in a poly(vinylidene fluoride-*co*-trifluoroethylene-*co*-chlorotrifluoroethylene)-*graft*-polystyrene graft vopolymer. Macromolecules. 2013;46:9698-711.

[24] Zhang S, Lee KH, Frisbie CD, Lodge TP. Ionic conductivity, capacitance, and viscoelastic properties of block copolymer-based ion gels. Macromolecules. 2011;44:940-9.

[25] Kim SH, Hong K, Xie W, Lee KH, Zhang S, Lodge TP, et al. Electrolyte-gated transistors for organic and printed electronics. Adv Mater. 2013;25:1822-46.

[26] Srinivasan S. Fuel cells: from Fundamentals to applications. New York: Springer; 2006. p. 27-92.

[27] Bockris JOM, Reddy AKN, Gamboa-Aldeco M, Modern electrochemistry: Fundamentals of electrodics, Vol. 2A, 2nd Ed. New York: Kluwer Academic; 2002. p. 771-1033.

[28] Zhang G. Allahyarov E, Zhu L. Polymer nanodielectrics: Current accomplishments and future challenges for electric energy storage. In: Li B. Jiao T, editor. Nano/micro-structured materials for energy and biomedical applications. Singapore: Springer; 2018. p.1-48.

[29] Nelson JK, Dielectric polymer nanocomposites. New York: Springer; 2010. 368 pp.

[30] Wang Q, Zhu L. Polymer nanocomposites for electrical energy storage. J Polym Sci, Part

B: Polym Phys. 2011;49:1421-9.

[31] Prateek, Thakur VK, Gupta RK. Recent progress on ferroelectric polymer-based nanocomposites for high energy density capacitors: Synthesis, dielectric properties, and future aspects. Chem Rev. 2016;116:4260-317.

[32] Kumar SK, Benicewicz BC, Vaia RA, Winey KI. 50th Anniversary perspective: Are polymer nanocomposites practical for applications? Macromolecules. 2017;50:714-31.

[33] Zhang X, Li BW, Dong LJ, Liu H, Chen W, Shen Y, et al. Superior energy storage performances of polymer nanocomposites via modification of filler/polymer interfaces. Adv Mater Interfaces. 2018;11:1800096/1-28.

[34] Tan DQ. Review of polymer-based nanodielectric exploration and film scale-up for advanced capacitors. Adv Funct Mater. 2019;29:1808567/1-23.

[35] Huang XY, Sun B, Zhu YK, Li ST, Jiang PK. High-*k* polymer nanocomposites with 1D filler for dielectric and energy storage applications. Prog Mater Sci. 2019;100:187-225.

[36] Allahyarov E, Lowen H, Zhu L. Dipole correlation effects on the local field and the effective dielectric constant in composite dielectrics containing high-*k* inclusions. Phys Chem Chem Phys. 2016;18:19103-17.

[37] Tseng JK, Yin K, Zhang Z, Mackey M, Baer E, Zhu L. Morphological effects on dielectric properties of poly(vinylidene fluoride-*co*-hexafluoropropylene) blends and multilayer films. Polymer. 2019;172:221-30.

[38] Zhang G, Brannum D, Dong D, Tang L, Allahyarov E, Tang S, et al. Interfacial polarization-induced loss mechanisms in polypropylene/$BaTiO_3$ nanocomposite dielectrics. Chem Mater. 2016;28:4646-60.

[39] Paniagua SA, Kim Y, Henry K, Kumar R, Perry JW, Marder SR. Surface-initiated

polymerization from barium titanate nanoparticles for hybrid dielectric capacitors. ACS Appl Mater Interfaces. 2014;6:3477-82.

[40] Calame JP. Finite difference simulations of permittivity and electric field statistics in ceramic-polymer composites for capacitor applications. J Appl Phys. 2006;99:084101/1-11.

[41] An L, Boggs SA, Callame JP. Energy storage in polymer films with high dielectric constant fillers. IEEE Electr Insul Mag. 2008;24:5-10.

[42] Dang ZM, Wu JB, Fan LZ, Nan CW. Dielectric behavior of Li and Ti co-doped NiO/PVDF composites. Chem Phys Lett. 2003;376:389-94.

[43] Arbatti M, Shan X, Cheng ZY. Ceramic-polymer composites with high dielectric constant. Adv Mater. 2007;19:1369-72.

[44] Dang ZM, Shen Y, Nan CW. Dielectric behavior of three-phase percolative Ni-$BaTiO_3$/polyvinylidene fluoride composites. Appl Phys Lett. 2002;81:4814-6.

[45] Grabowski CA, Koerner H, Meth JS, Dang A, Hui CM, Matyjaszewski K, et al. Performance of Dielectric Nanocomposites: Matrix-Free, Hairy Nanoparticle Assemblies and Amorphous Polymer-Nanoparticle Blends. ACS Appl Mater Interfaces. 2014;6:21500-9.

[46] Grabowski CA, Fillery SP, Westing NM, Chi CZ, Meth JS, Durstock MF, et al. Dielectric breakdown in silica-amorphous polymer nanocomposite films: The role of the polymer matrix. ACS Appl Mater Interfaces. 2013;5:5486-92.

[47] Singha S, Thomas MJ. Dielectric properties of epoxy nanocomposites. IEEE Trans Dielectr Electr Insul. 2008;15:12-23.

[48] Li J, Seok SI, Chu B, Dogan F, Zhang Q, Wang Q. Nanocomposites of ferroelectric

polymers with TiO_2 nanoparticles exhibiting significantly enhanced electrical energy density. Adv Mater. 2009;21:217-21.

[49] Thakur Y, Zhang T, Iacob C, Yang T, Bernholc J, Chen LQ, et al. Enhancement of the dielectric response in polymer nanocomposites with low dielectric constant fillers. Nanoscale. 2017;9:10992-7.

[50] Wang W, Min D, Li S. Understanding the conduction and breakdown properties of polyethylene nanodielectrics: Effect of deep traps. IEEE Trans Dielectr Electr Insul. 2016;23:564-72.

[51] Thakur Y, Lean MH, Zhang QM. Reducing conduction losses in high energy density polymer using nanocomposites. Appl Phys Lett. 2017;110:122905/1-5.

[52] Lu J, Moon KS, Xu J, Wong CP. Synthesis and dielectric properties of novel high-K polymer composites containing in-situ formed silver nanoparticles for embedded capacitor applications. J Mater Chem. 2006;16:1543-8.

[53] Kofod G, Risse S, Stoyanov H, McCarthy DN, Sokolov S, Kraehnert R. Broad-spectrum enhancement of polymer composite dielectric constant at ultralow volume fractions of silica-supported copper nanoparticles. ACS Nano. 2011;5:1623-9.

[54] Fredin LA, Li Z, Lanagan MT, Ratner MA, Marks TJ. Substantial recoverable energy storage in percolative metallic aluminum-polypropylene nanocomposites. Adv Funct Mater. 2013;23:3560-9.

[55] Dang ZM, Wang L, Yin Y, Zhang Q, Lei QQ. Giant dielectric permittivities in functionalized carbon-nanotube/electroactive-polymer nanocomposites. Adv Mater. 2007;19:852-7.

[56] He F, Lau S, Chan HL, Fan J. High dielectric permittivity and low percolation threshold in

nanocomposites based on poly(vinylidene fluoride) and exfoliated graphite nanoplates. Adv Mater. 2009;21:710-5.

[57] Yousefi N, Sun X, Lin X, Shen X, Jia J, Zhang B, et al. Highly aligned graphene/polymer nanocomposites with excellent dielectric properties for high-performance electromagnetic interference shielding. Adv Mater. 2014;26:5480-7.

[58] Nan CW. Physics of inhomogeneous inorganic materials. Prog Mater Sci. 1993;37:1-116.

[59] Nan CW, Shen Y, Ma J. Physical properties of composites near percolation. Annu Rev Mater Res. 2010;40:131-51.

[60] Zhang G, Li Y, Tang S, Thompson RD, Zhu L. The role of field electron emission in polypropylene/aluminum nanodielectrics under high electric fields. ACS Appl Mater Interfaces. 2017;9:10106-19.

[61] Sheng P, Abeles B. Voltage-induced tunneling conduction in granular metals at low temperatures. Phys Rev Lett. 1972;28:34-7.

[62] Laurent C, Kay E, Souag N. Dielectric breakdown of polymer films containing metal clusters. J Appl Phys. 1988;64:336-43.

[63] Webb AJ, Bloor D, Szablewski M, Atkinson D. Temperature dependence of electrical transport in a pressure-sensitive nanocomposite. ACS Appl Mater Interfaces. 2014;6:12573-80.

[64] Paredes-Madrid L, Palacio CA, Matute A, Parra Vargas CA. Underlying physics of conductive polymer composites and force sensing resistors (FSRs) under static loading conditions. Sensors. 2017;17:2108/1-34.

[65] Liu X, Osaka T. All-solid-state electric double-layer capacitor with isotropic high-density graphite electrode and polyethylene oxide/$LiClO_4$ polymer electrolyte. J Electrochem Soc.

1996;143:3982-6.

[66] Cho JH, Lee J, Xia Y, Kim B, He Y, Renn MJ, et al. Printable ion-gel gate dielectrics for low-voltage polymer thin-film transistors on plastic. Nat Mater. 2008;7:900-6.

[67] Lee KH, Zhang S, Lodge TP, Frisbie CD. Electrical impedance of spin-coatable ion gel films. J Phys Chem B. 2011;115:3315-21.

[68] Sinha JK. Modified Sawyer and Tower circuit for investigation of ferroelectric samples. J Sci Instrum. 1965;42:696-8.

[69] Li Y, Ho J, Wang J, Li ZM, Zhong GJ, Zhu L. Understanding nonlinear dielectric properties in a biaxially oriented poly(vinylidene fluoride) film at both low and high electric fields. ACS Appl Mater Interfaces. 2016;8:455-65.

[70] Franceschetti DR, Macdonald JR. Numerical-analysis of electrical response: Biased small-signal a.c. response for systems with one or two blocking electrodes. J Electroanal Chem. 1979;100:583-605.

[71] Franceschetti DR, Macdonald JR. Numerical-analysis of electrical response: Statics and dynamics of space-charge regions at blocking electrodes. J Appl Phys. 1979;50:291-302.

[72] Havrilia.S, Negami S. A complex plane representation of dielectric and mechanical relaxation processes in some polymers. Polymer. 1967;8:161-210.

[73] Fukasawa T, Sato T, Watanabe J, Hama Y, Kunz W, Buchner R. Relation between dielectric and low-frequency Raman spectra of hydrogen-bond liquids. Phys Rev Lett. 2005;95:197802/1-4.

[74] Leader GR, Gormile JF. The dielectric constant of N-methylamides. J Am Chem Soc. 1951;73:5731-3.

[75] Wang CC, Pilania G, Boggs SA, Kumar S, Breneman C, Ramprasad R. Computational

strategies for polymer dielectrics design. Polymer. 2014;55:979-88.

[76] Wang C, Zhang Z, Pejic S, Li R, Fukuto M, Zhu L, et al. High dielectric constant semiconducting poly(3-alkylthiophene)s from side chain modification with polar sulfinyl and sulfonyl groups. Macromolecules. 2018;51:9368-81.

[77] Zhao Z, Zhang Z, Pejic S, Zhang G, Zhu Y, Liu H, et al. Synergistic dielectric and semiconducting properties in fluorescein monopotassium salt random copolymers. Polymer. 2017;114:189-98.

[78] Mark JE. Polymer data handbook. 2nd ed. Oxford: Oxford University Press; 2009. 1250 pp.

[79] Kane DE. The relationship between the dielectric constant and water-vapor accessibility of cellulose. J Polym Sci. 1955;18:405-10.

[80] Millefiori S, Alparone A, Milleflori A, Vanella A. Electronic and vibrational polarizabilities of the twenty naturally occurring amino acids. Biophys Chem. 2008;132:139-47.

[81] Wu S, Li W, Lin M, Burlingame Q, Chen Q, Payzant A, et al. Aromatic polythiourea dielectrics with ultrahigh breakdown field strength, low dielectric loss, and high electric energy density. Adv Mater. 2013;25:1734-8.

[82] Wu S, Burlingame Q, Cheng ZX, Lin M, Zhang QM. Strongly dipolar polythiourea and polyurea dielectrics with high electrical breakdown, low loss, and high electrical energy density. J Electron Mater. 2014;43:4548-51.

[83] Thakur Y, Lin M, Wu S, Cheng Z, Jeong DY, Zhang QM. Tailoring the dipole properties in dielectric polymers to realize high energy density with high breakdown strength and low dielectric loss. J Appl Phys. 2015;117:114104/1-6.

[84] Thakur Y, Zhang B, Dong R, Lu W, Iacob C, Runt J, et al. Generating high dielectric

constant blends from lower dielectric constant dipolar polymers using nanostructure engineering. Nano Energy. 2017;32:73-9.

[85] Nalwa HS, Dalton LR, Vasudevan P. Dielectric-properties of copper-phthalocyanine polymer. Eur Polym J. 1985;21:943-7.

[86] Nalwa HS. Handbook of low and high dielectric constant materials and their applications. Vol. 1. San Diego: Academic Press; 1999. 569 pp.

[87] Zhang QM, Li H, Poh M, Xia F, Cheng ZY, Xu H, et al. An all-organic composite actuator material with a high dielectric constant. Nature. 2002;419:284-7.

[88] Wang JW, Shen QD, Yang CZ, Zhang QM. High dielectric constant composite of P(VDF-TrFE) with grafted copper phthalocyanine oligomer. Macromolecules. 2004;37:2294-8.

[89] Wang JW, Shen QD, Bao HM, Yang CZ, Zhang QM. Microstructure and dielectric properties of P(VDF-TrFE-CFE) with partially grafted copper phthalocyanine oligomer. Macromolecules. 2005;38:2247-52.

[90] Chen L, Ding Y, Yang T, Wan C, Hou H. Synthesis and properties of a high dielectric constant copolymer of a copper phthalocyanine oligomer grafted to amino-capped polyimide. J Mater Chem C. 2017;5:8371-5.

[91] Wang J, Guan F, Cui L, Pan J, Wang Q, Zhu L. Achieving high electric energy storage in a polymer nanocomposite at low filling ratios using a highly polarizable phthalocyanine interphase. J Polym Sci, Part B: Polym Phys. 2014;52:1669-80.

[92] Boston DR, Bailar JC. Phthalocyanine derivatives from 1,2,4,5-tetracyanobenzene or pyromellitic dianhydride and metal-salts. Inorg Chem. 1972;11:1578-83.

[93] Achar BN, Fohlen GM, Parker JA. Phthalocyanine polymers. 2. Synthesis and characterization of some metal phthalocyanine sheet oligomers. J Polym Sci, Part A: Polym

Chem. 1982;20:1785-90.

[94] Bobnar V, Levstik A, Huang C, Zhang QM. Intrinsic dielectric properties and charge transport in oligomers of organic semiconductor copper phthalocyanine. Phys Rev B. 2005;71: 041202/1-4.

[95] Opris DM, Nuesch F, Lowe C, Molberg M, Nagel M. Synthesis, characterization, and dielectric properties of phthalocyanines with ester and carboxylic acid functionalities. Chem Mater. 2008;20:6889-96.

[96] Mezei G, Venter AR, Kreft JW, Urech AA, Mouch NR. Monomeric, not tetrameric species are responsible for the colossal dielectric constant of copper phthalocyanine derived from pyromellitic dianhydride. RSC Adv. 2012;2:10466-9.

[97] Mezei G. Comment on "Synthesis and properties of high dielectric constant copolymer of a copper phthalocyanine oligomer grafted to amino-capped polyimide" by L. Chen, Y. Ding, T. Yang, C. Wan and H. Hou, J. Mater. Chem. C, 2017, 5, 8371. J Mater Chem C. 2019;7:4887-91.

[98] Hamam KJ, Al-Amar MM, Mezei G, Guda R, Burns C. High dielectric constant response of modified copper phthalocyanine. J Mol Liq. 2014;199:324-9.

[99] Islam MS, Qiao Y, Tang C, Ploehn HJ. Terthiophene-containing copolymers and homopolymer blends as high-performance dielectric materials. ACS Appl Mater Interfaces. 2015;7:1967-77.

[100] Elton DC, Fernandez-Serra MV. Polar nanoregions in water: A study of the dielectric properties of TIP4P/2005, TIP4P/2005f and TTM3F. J Chem Phys. 2014;140:124504/1-12.

[101] Yang L, Ho J, Allahyarov E, Mu R, Zhu L. Semicrystalline structure dielectric property relationship and electrical conduction in a biaxially oriented poly(vinylidene fluoride) film

under high electric fields and high temperatures. ACS Appl Mater Interfaces. 2015;7:19894-905.

[102] Lovinger AJ. Ferroelectric polymers. Science. 1983;220:1115-21.

[103] Zhu L, Wang Q. Novel ferroelectric polymers for high energy density and low loss dielectrics. Macromolecules. 2012;45:2937-54.

[104] Nakhmanson SM, Nardelli MB, Bernholc J. Collective polarization effects in beta-polyvinylidene fluoride and its copolymers with tri- and tetrafluoroethylene. Phys Rev B. 2005;72:115210/1-8.

[105] Aljishi R, Taylor PL. Equilibrium polarization and piezoelectric and pyroelectric coefficients in poly(vinylidene fluoride). J Appl Phys. 1985;57:902-5.

[106] Tashiro K. Crystal structure and phase transition of PVDF and related copolymers. In: Nalwa HS, editor. Ferroelectric polymers: Chemistry, physics, and applications. New York: Marcel Dekker; 1995. p. 63-181.

[107] Li M, Wondergem HJ, Spijkman MJ, Asadi K, Katsouras I, Blom PWM, et al. Revisiting the δ-phase of poly(vinylidene fluoride) for solution-processed ferroelectric thin films. Nat Mater. 2013;12:433-8.

[108] Boulesteix C, Varnier F, Llebaria A, Husson E. Numerical determination of the local ordering of $PbMg_{1/3}Nb_{2/3}O_3$ (PMN) from high resolution electron microscopy images. J Solid State Chem. 1994;108:141-7.

[109] Samara GA. The relaxational properties of compositionally disordered ABO_3 perovskites. J Phys: Condens Matter. 2003;15:R367-R411.

[110] Bokov AA, Ye ZG. Recent progress in relaxor ferroelectrics with perovskite structure. J Mater Sci. 2006;41:31-52.

[111] Furukawa T. Structure and functional properties of ferroelectric polymers. Adv Colloid Interface Sci. 1997;71-2:183-208.

[112] Wunderlich B. Macromolecular Physics, Vol. 1: Crystal structure, morphology, and defects. New York,: Academic Press; 1973. 549 pp.

[113] Yang L, Li X, Allahyarov E, Taylor PL, Zhang QM, Zhu L. Novel polymer ferroelectric behavior via crystal isomorphism and the nanoconfinement effect. Polymer. 2013;54:1709-28.

[114] Hattori T, Hikosaka M, Ohigashi H. The crystallization behaviour and phase diagram of extended-chain crystals of poly(vinylidene fluoride) under high pressure. Polymer. 1996;37:85-91.

[115] Hattori T, Watanabe T, Akama S, Hikosaka M, Ohigashi H. The high-pressure crystallization behaviours and piezoelectricity of extended chain lamellar crystals of vinylidene fluoride trifluoroethylene copolymers with high molar content of vinylidene fluoride. Polymer. 1997;38:3505-11.

[116] Huang Y, Xu J-Z, Soulestin T, Dos Santos FD, Li R, Fukuto M, et al. Can relaxor ferroelectric behavior be realized for poly(vinylidene fluoride-*co*-chlorotrifluoroethylene) [P(VDF-CTFE)] random copolymers by inclusion of CTFE Units in PVDF crystals? Macromolecules. 2018;51:5460-72.

[117] Chu B, Zhou X, Ren K, Neese B, Lin M, Wang Q, et al. A dielectric polymer with high electric energy density and fast discharge speed. Science. 2006;313:334-6.

[118] Zhou X, Chu B, Neese B, Lin M, Zhang QM. Electrical energy density and discharge characteristics of a poly(vinylidene fluoride-chlorotrifluoroethylene) copolymer. IEEE Trans Dielectr Electr Insul. 2007;14:1133-8.

[119] Zhou X, Zhao X, Suo Z, Zou C, Runt J, Liu S, et al. Electrical breakdown and ultrahigh electrical energy density in poly(vinylidene fluoride-hexafluoropropylene) copolymer. Appl Phys Lett. 2009;94:162901/1-3.

[120] Lovinger AJ. Polymorphic transformations in ferroelectric copolymers of vinylidene fluoride induced by electron-irradiation. Macromolecules. 1985;18:910-8.

[121] Zhang QM, Bharti V, Zhao X. Giant electrostriction and relaxor ferroelectric behavior in electron-irradiated poly(vinylidene fluoride-trifluoroethylene) copolymer. Science. 1998;280:2101-4.

[122] Bharti V, Zhao XZ, Zhang QM, Romotowski T, Tito F, Ting R. Ultrahigh field induced strain and polarization response in electron irradiated poly(vinylidene fluoride-trifluoroethylene) copolymer. Mater Res Innovations. 1998;2:57-63.

[123] Chung TC, Petchsuk A. Ferroelectric VDF/TrFE/CTFE terpolymers: Synthesis and electric properties. Proc. SPIE, Smart Structures and Materials 2001: Electroactive Polymer Actuators and Devices. 2001;4329:117-24.

[124] Chung TC, Petchsuk A. Synthesis and properties of ferroelectric fluoroterpolymers with Curie transition at ambient temperature. Macromolecules. 2002;35:7678-84.

[125] Soulestin T, Ladmiral V, Dos Santos FD, Ameduri B. Vinylidene fluoride- and trifluoroethylene-containing fluorinated electroactive copolymers. How does chemistry impact properties? Prog Polym Sci. 2017;72:16-60.

[126] Ameduri B. From vinylidene fluoride (VDF) to the applications of VDF-containing polymers and copolymers: Recent developments and future trends. Chem Rev. 2009;109:6632-86.

[127] Yang L, Tyburski BA, Domingues Dos Santos F, Endoh MK, Koga T, Huang D, et al.

Relaxor ferroelectric behavior from strong physical pinning in a poly(vinylidene fluoride-*co*-trifluoroethylene-*co*-chlorotrifluoroethylene) random terpolymer. Macromolecules. 2014;47:8119-25.

[128] Gadinski MR, Li Q, Zhang G, Zhang X, Wang Q. Understanding of relaxor ferroelectric behavior of poly(vinylidene fluoride-trifluoroethylene-chlorotrifluoroethylene) terpolymers. Macromolecules. 2015;48:2731-9.

[129] Su R, Tseng JK, Lu MS, Lin M, Fu Q, Zhu L. Ferroelectric behavior in the high temperature paraelectric phase in a poly(vinylidene fluoride-co-trifluoroethylene) random copolymer. Polymer. 2012;53:728-39.

[130] Zhang Z, Litt MH, Zhu L. Understanding the paraelectric double hysteresis loop behavior in mesomorphic even-numbered nylons at high temperatures. Macromolecules. 2017;50:5816-29.

[131] Fried JR. Sub-Tg transitions. In: Mark JE, editor. Physical properties of polymers handbook. New York: Springer; 2007. p. 161-175.

[132] Treufeld I, Wang DH, Kurish BA, Tan LS, Zhu L. Enhancing electrical energy storage using polar polyimides with nitrile groups directly attached to the main chain. J Mater Chem A. 2014;2:20683-96.

[133] Wang DH, Kurish BA, Treufeld I, Zhu L, Tan LS. Synthesis and characterization of high nitrile content polyimides as dielectric films for electrical energy storage. J Polym Sci, Part A: Polym Chem. 2015;53:422-36.

[134] Yang T, Xu W, Peng X, Hou H. Crown ether-containing polyimides with high dielectric constant. RSC Adv. 2017;7:23309-12.

[135] Zhang Z, Litt MH, Zhu L. Nature of ferroelectric behavior in main-chain dipolar glass

nylons: Cooperative segmental motion induced by high poling electric field. Macromolecules. 2018;51:1967-77.

[136] Yuan X, Matsuyama Y, Chung TCM. Synthesis of functionalized isotactic polypropylene dielectrics for electric energy storage applications. Macromolecules. 2010;43:4011-5.

[137] Stoops WN. The dielectric properties of cellulose. J Am Chem Soc. 1934;56:1480-3.

[138] Lao J, Xie H, Shi Z, Li G, Li B, Hu GH, et al. Flexible regenerated cellulose/boron nitride nanosheet high-temperature dielectric nanocomposite flms with high energy density and breakdown strength. ACS Sustainable Chem Eng. 2018;6:7151-8.

[139] Bendler JT, Boyles DA, Edmondson CA, Filipova T, Fontanella JJ, Westgate MA, et al. Dielectric properties of bisphenol A polycarbonate and its tethered nitrile analogue. Macromolecules. 2013;46:4024-33.

[140] Vandeleur RHM. An extended analysis of the dielectric properties of poly[(2-cyanoethyl vinyl ether)-*co*-(vinyl alcohol)]. Polymer. 1994;35:2691-700.

[141] Bedekar BA, Tsujii Y, Ide N, Kita Y, Fukuda T, Miyamoto T. Dielectric relaxation of cyanoethylated poly(2,3-dihydroxypropyl methacrylate). Polymer. 1995;36:4735-40.

[142] Sato T, Tsujii Y, Kita Y, Fukuda T, Miyamoto T. Dielectric relaxation of liquid crystalline cyanoethylated O-(2,3-dihydroxypropyl)cellulose. Macromolecules. 1991;24:4691-7.

[143] Tasaka S, Inagaki N, Miyata S, Chiba T. Electrical properties of cyanoethylated polysaccharides. Sen′i Gakkaishi. 1988;44:546-50.

[144] Wei J, Zhang Z, Tseng JK, Treufeld I, Liu X, Litt MH, et al. Achieving high dielectric constant and low loss property in a dipolar glass polymer containing strongly dipolar and small-sized sulfone groups. ACS Appl Mater Interfaces. 2015;7:5248-57.

[145] Wang Y, Huang X, Li T, Wang Z, Li L, Guo X, et al. Novel crosslinkable high-k copolymer

dielectrics for high-energy-density capacitors and organic field-effect transistor applications. J Mater Chem A. 2017;5:20737-46.

[146] Zhu YF, Zhang Z, Litt MH, Zhu L. High dielectric constant sulfonyl-containing dipolar glass polymers with enhanced orientational polarization. Macromolecules. 2018;51:6257-66.

[147] Zhang Z, Wang DH, Litt MH, Tan LS, Zhu L. High-temperature and high-energy-density dipolar glass polymers based on sulfonylated poly(2,6-dimethyl-1,4-phenylene oxide). Angew Chem Int Ed. 2018;57:1528-31.

[148] Zhang Z, Zheng J, Premasiri K, Kwok M-H, Li Q, Li R, et al. High-κ polymers of intrinsic microporosity: A new class of high temperature and low loss dielectrics for printed electronics. Mater Horiz. 2020;7: DOI: 10.1039/C9MH01261C.

[149] Seanor DA. Electronic and ionicconductivity in nylon 66. J Polym Sci A-2: Polym. Phys. 1968;6:463-77.

[150] Eberle G, Schmidt H, Eisenmenger W. Influence of poling conditions on the gas emission of PVDF. IEEE 1993 Confr Electr Insul Dielectr Phenom. 1993; p. 263-8.

[151] a) Baer E, Hiltner A, Shirk JS, Wolak MA. Multilayer polymer dielectric film. US 20100172066A1, 2010. b) Baer E, Hiltner A, Shirk JS, Wolak MA. Multilayer polymer dielectric film. US 20140160623A1, 2014.

[152] Langhe D, Ponting M. Manufacturing and novel applications of multilayer polymer films. Amsterdam: Elsevier; 2015. 250 pp.

[153] Tseng JK, Tang S, Zhou Z, Mackey M, Carr JM, Mu R, et al. Interfacial polarization and layer thickness effect on electrical insulation in multilayered polysulfone/poly(vinylidene fluoride) films. Polymer. 2014;55:8-14.

[154] Chen X, Tseng J-K, Treufeld I, Mackey M, Schuele DE, Li R, et al. Enhanced dielectric properties due to space charge-induced interfacial polarization in multilayer polymer films. J Mater Chem C. 2017;5:10417-26.

[155] Mackey M, Hiltner A, Baer E, Flandin L, Wolak MA, Shirk JS. Enhanced breakdown strength of multilayered films fabricated by forced assembly microlayer coextrusion. J Phys D: Appl Phys. 2009;42:175304/1-12.

[156] Yin K, Zhang J, Li Z, Feng J, Zhang C, Chen X, et al. Polymer multilayer films for high temperature capacitor application. J Appl Polym Sci. 2019;136:47535/1-8.

[157] Li Z, Chen X, Zhang C, Baer E, Langhe D, Ponting M, et al. High dielectric constant polycarbonate/nylon multilayer films capacitors with self-healing capability. ACS Appl Polym Mater. 2019;1:867-75.

[158] Chiu FC. A review on conduction mechanisms in dielectric films. Adv Mater Sci Eng. 2014; 7:1-18.

[159] Dissado LA, Fothergill JC. Electrical degradation and breakdown in polymers. London: P. Peregrinus; 1992. 601 pp.

[160] Mayoux C. Degradation of insulating materials under electrical stress. IEEE Trans Dielectr Electr Insul. 2000;7:590-601.

[161] Reed CW, Cichanowski SW. The fundamentals of aging in HV polymer-film capacitors. IEEE Trans Dielectr Electr Insul. 1994;1:904-22.